UNIVERSITAT POLITÈCNICA DE VALÈNCIA

Departamento de Ingeniería Mecánica y de Materiales

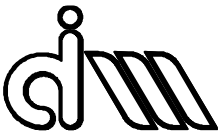

Trabajo Fin de Máster en Ingeniería Mecánica

"HiLiTe2" High-Speed Linear Test Rig 2

Presentado por: D. Luis Urueña Pérez
Dirigido por: Dr. D. Francisco David Denia Guzmán
Codirigido por: Dr. D. Matthias Wangenheim

Valencia, Marzo de 2017

Thanks to:

Dr. Matthias Wangenheim to give me the chance to work in this inspiring project. Thanks to Tim Linke who was my colleague in the institute. We discussed about some different ideas of the project and finally a great result was achieved.

I would like also to acknowledge the Universitat Politècnica de València to give me the chance to participate in this Erasmus program and my tutor in Spain, Francisco David Denia Guzmán, to understand and facilitate the presentation of my Master's Thesis.

Abstract

The “HiLiTe“ is designed to investigate frictional behaviour of rubber samples on a variety of test surfaces.
Properties:

- Test Samples: rubber tire samples
- Sliding speed: 0.1 - 10 m / s
- Normal force applied: 100 – 2000 N
- Length of test tracks: 5 m
- Temperatures: -20 °C ... +40 °C
- Additional equipment: Thermal camera, high-speed camera.
- Tests on asphalt, concrete, snow & ice possible.

The main problem with the current design is that it does not adapt to the specifications required by the new tests.
The present project will seek to address these problems through the achievement of the goals set out below:

- To increase the normal force (2000 N).
- New mechanical design that is able to pull up the chassis with the pressure of 6 bar and stroke of 40 mm.
- To carry out a new mechanical design that is capable of withstanding the normal load of 2000 N.
- Introduction of a new linear potentiometer with a stroke of 40 mm.
- New design of the sample holder.

Key words:

HiLiTe2 “High-Speed Linear Test Rig 2”, bellow cylinder, carriage, frame, piston, linear potentiometer, tire, INVENTOR.

Resumen.

El “HiLiTe” es un banco de pruebas donde se realizan ensayos de fricción de la goma del neumático. Pruebas sobre asfalto, hormigón, nieve y hielo.
Las nuevas condiciones a cumplir son:
- Muestras: muestras de goma de neumático
- Velocidad: 0.1 - 10 m/s
- Fuerza Normal aplicada 100 – 2000 N
- Longitud de la carretera: 5 m
- Temperaturas: -20ºC……+40ºC
- Equipo adicional: cámara térmica y cámara para alta velocidad.

Los principales problemas que plantea la actual máquina es que no está adaptada a los actuales requerimientos de ensayo.

En el presente proyecto se tratará de solucionar estos problemas mediante la consecución de los objetivos que se establecen a continuación:

- Aumentar la fuerza normal aplicada hasta 2000 N.
- Nuevo diseño mecánico que sea capaz de subir el chasis con la presión de 6 bar y con un recorrido de 40 mm.
- Realizar un nuevo diseño mecánico que sea capaz de soportar la fuerza normal de 2000 N.
- Introducción de un nuevo potenciómetro lineal con un recorrido de 40mm.
- Nuevo diseño del portamuestras.

Palabras clave:
HiLiTe2 “High-Speed Linear Test Rig 2”, cilindro neumático, carro, armazón, pistón, potenciómetro lineal, neumático, INVENTOR

Resum:

Aquest banc de proves serveix per a realitzar assajos de fricció de la goma del pneumàtic. Proves asfalt, formigó, neu i gel.
Les noves condicions a complir són:
- Mostres: mostres de goma de pneumàtic
- Velocitat: 0.1 - 10 m / s
- Força Normal aplicada 100 - 2000N
- Longitud de la carretera: 5 m
- Temperatures: -20ºC ..... + 40ºC
- Equip adicional: càmera tèrmica i càmera per a alta velocitat.

Els principals problemes que planteja l'actual màquina és que no està adaptada als actuals requeriments d'assaig.

En el present projecte es tractarà de solucionar aquests problemes mitjançant la consecució dels objectius que s'estableixen a continuació:

- Augmentar la força normal aplicada fins 2000 N.
- Nou disseny mecànic que siga capaç de pujar el xassís amb la pressió de 6 bar i amb un recorregut de 40 mm.
- Realitzar un nou disseny mecànic que siga capaç de suportar la força normal de 2000 N.
- Introducció d'un nou potenciòmetre lineal amb un recorregut de 40 mm.
- Nou disseny del portamostres.

Paraules clau:

HiLiTe2 "High-Speed Linear Test Rig 2", cilindre pneumàtic, carro, carcassa, pistó, potenciòmetre lineal, pneumàtic, INVENTOR

Contents

Index of the images

Tables Index

Graphic Index

Equation Index

Abbreviations

HiLiTe: High-Speed Linear Test Rig 2
IDS: Institut für Dynamik und Schwingungen - Institute of dynamics and vibrations

CHAPTER 1: Introduction and goals

Chapter 1: Introduction and goals

1.1. Introduction and goals

This Project has taken place at the Leibniz Universität Hannover, in the IDS (Institut für Dynamik und Schwingungen). The main goal was to design a new "HiLiTe2" in order to achieve the new restrictions.

The first chapter of this document corresponds to the introduction.
It presents the structure of the project in chapters and briefly explains the content of each one of them.

1.2. Project statement, justification and goals.

This second chapter explains the statement, goals and justification of the project. The chapter begins with a brief explanation of the current situation.
After this block, the project is justified.
To finalize the chapter, the goals we try to achieve in the present project are detailed. The tasks carried out in the project in order to solve the problems of the new conditions are also detailed.

1.3. Background and Theory Concepts

This chapter is divided in three subchapters: briefly explanation of the "HiLiTe", one example of the results obtained through it. Finally basic theory concepts are explained (force transducer and bearings).

1.4. New design and description of the technical solutions.

This chapter will be the core of this project. It details all the solutions and modifications that have been made to achieve the goals. INVENTOR has been used as a 3D software (CAD) and ANSYS WORKBENCH (CAE).

In the first block the chosen pneumatic cylinders are detailed. After that all the design carried out in the frame to make it possible is detailed.

The second block shows the new design to pull up the chassis. It is achieved through two pistons introduced symmetrically in the overall design.

Finally, the third block of this chapter details the new design system to support the chassis under the maximum load and the design to introduce the linear potentiometer needed for tests under snow conditions.

1.5. Calculations and simulations

In this chapter, all the calculations necessary for the realization of the project will be presented.

In the first block, an analysis of the bolts has been done in order to check that they achieve the specifications. Moreover the tolerances demanded have been calculated.

Secondly, FEA has been done to make the new design with the lowest weight possible to achieve the acceleration goal.

Finally, the horizontal and vertical dynamic load to be supported for the next steps of the project have been calculated.

1.6. Conclusions and future lines.

This chapter is the last chapter of the document. It begins with a review of the goals that were pursued with the realization of this project, to later study the conclusions obtained. Finally, a set of future lines of research will be presented due to the fact that I am going to continue working in the present project.

CHAPTER 2: Project statement, justification and goals.

CHAPTER 2: Project statement, justification and goals.

2.1.-Project statement

This Project has been taken place at the Leibniz Universität Hannover, in the IDS (Institut für Dynamik und Schwingungen). It has a test rig "HiLiTe" in order to make frictional tests to private companies such as Continental or Airbus.

The actual "HiLiTe" has an old design which doesn't satisfy the new restrictions for the current tests that the companies demand.
The main problem is that it cannot achieved a normal load of 2000 N. Moreover this design cannot pull up the chassis when the compressed air in the circuit is above 5 bar.

2.2.-Justification of the project

This Master Thesis was proposed by the Leibniz Universität Hannover under the Erasmus Program.
The proposal was born from the current need to modify the "HiLiTe" to improve it and adapt it to the new market needs.

2.3.-Goals of the present project

The main goal was modify the "HiLiTe" to improve it and adapt it to the new restrictions.

These changes are explained through the next goals to be achieved:

- Increase the normal force (2000 N).
- New mechanical design that is able to pull up the chassis with the pressure of 6 bar and stroke of 40 mm.
- Carry out a new mechanical design that is capable of withstanding the normal load of 2000 N.
- Introduction of a new linear potentiometer with a stroke of 40 mm.
- New design of the sample holder.

All these goals have been achieved with the space and manufacturing restrictions taking into account.

CHAPTER 3: Background and Theory Concepts

CHAPTER 3: Background and Theory Concepts

This chapter is divided in three subchapters: briefly explanation of the "HiLiTe", one example of the results obtained through it. Finally basic theory concepts are explained (force transducer and bearings).

3.1.-"HiLiTe" (High-Speed Linear Test Rig)

As it was explained above, the "HiLiTe" is designed to investigate frictional behaviour of rubber samples on a variety of test surfaces.
Properties:

- Test Samples: rubber tire samples
- Sliding speed: 0.1 - 10 m / s
- Normal force applied: 100 – 1000 N
- Length of test tracks: 5 m
- Temperatures: -20 °C ... +40 °C
- Additional equipment: Thermal camera, high-speed camera.
- Tests on asphalt, concrete, snow & ice possible.

This test rig is situated inside the "Institut für Dynamik und Schwingungen" (IDS). It is located in the laboratories. Most of the tests are demanded by companies such as Continental or Airbus.

In the following images the current "HiLiTe" and specifications are shown.

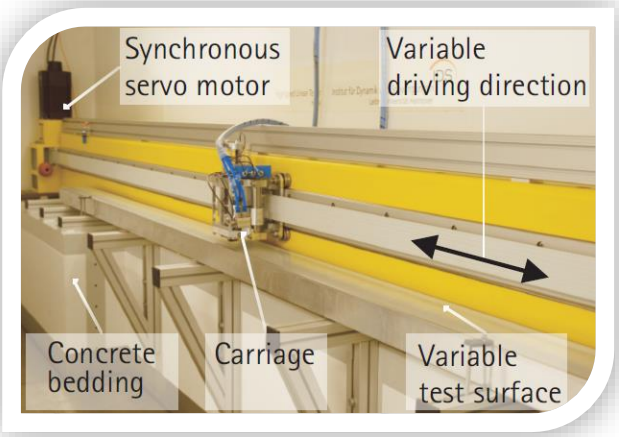

Image 1. - HiLiTe

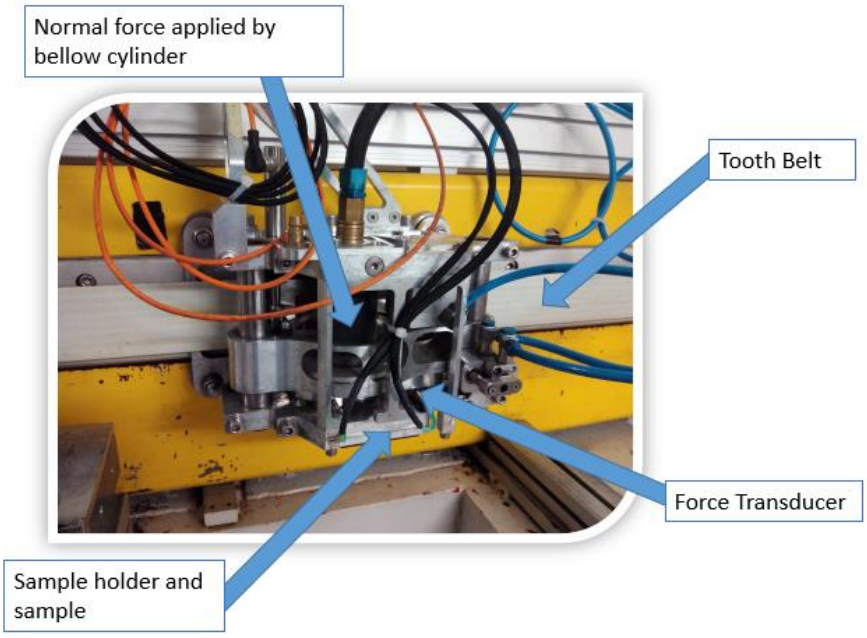

Image 2. - HiLiTe - Carriage

In the above picture it is shown how is the actual design.
This design is not symetric, thereby the load is not applied in the center. This characteristic causes problems in the distribution of loads and vibrations.
In addition, there is only one piston for pull up the chasis. It has not the necessary force to pull up the chassis with the pressure of 6 bar.

This is a serious problem since you have to manually change the pressure in the circuit to be able to back the carriage. If this step is forgotten, the carriage hits the road and the test is useless.

With the actual design it is necessary to unscrew a lot of bolts to take out the bellow cylinder.

The chassis is guide through two hollow shafts and two linear ball bearings which support the dynamic load.

The force sensor assembly is attached to the chassis. The theoretical explanation is shown below.

3.2.-Results obtained through "HiLiTe"

3.2.1.- Asphalt

In the graphics bellow is shown the Normal load (FN) and Frictional load (FR) which are measure through the force transducer, due to the fact that it can measure the force in 3 axis as it is explained in the theory's chapter.
Each test is repeated 10 times to achieve the average value.
In this test the sliding distance is 30mm. However, 5m can be achieved.

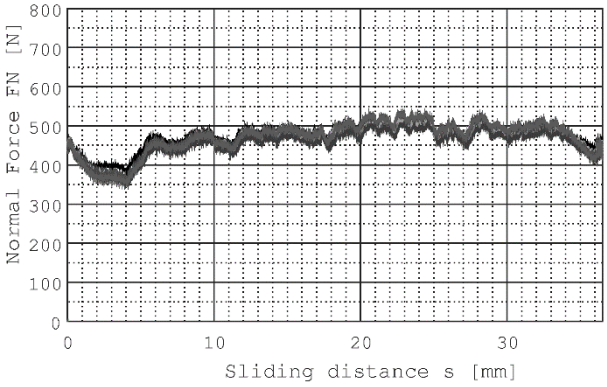

Graphic 1. - Normal Force FN (N)

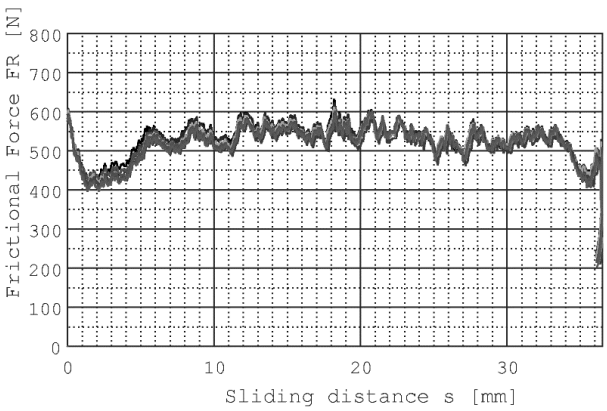

Graphic 2. - Frictional Force FR (N)

Once the force transducer has both component forces, the friction coefficient is calculated using the formula below. As it is showed in the graphic, the average value is 1.2. This is a really high value due to the fact that this test is in asphalt. After this results, a frictional coefficient value of 2 has been taken for calculations.

$$\mu = \frac{FN}{FR}$$

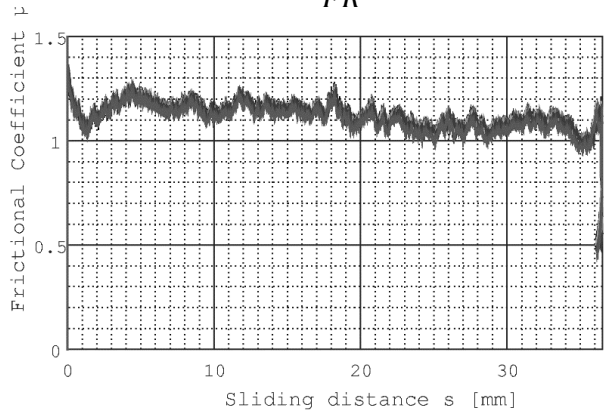

Graphic 3. - Frictional coefficient

Finally, the speed is measure directly from de motor. In this case the speed is 0.25m/s. However 10m/s can be achieved.

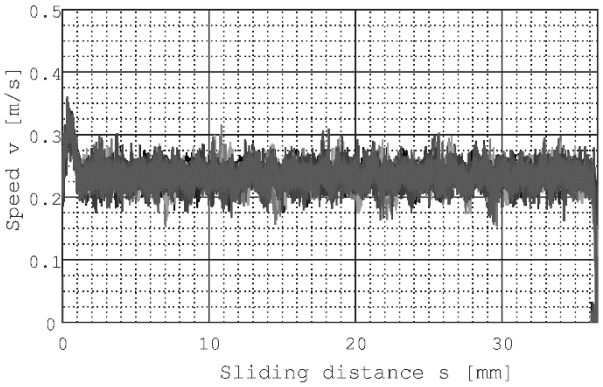

Graphic 4. - Speed (m/s)

3.2.2.- Test under snow conditions

In the laboratories there is one chamber where it is possible to make snow to create a snow path.
Moreover as it is shown in the specifications the temperatures in the "HiLiTe" go between -20……+40ºC.
In the graphic bellow it is shown 3 different test.
Each point is obtained after 10 repetitions.

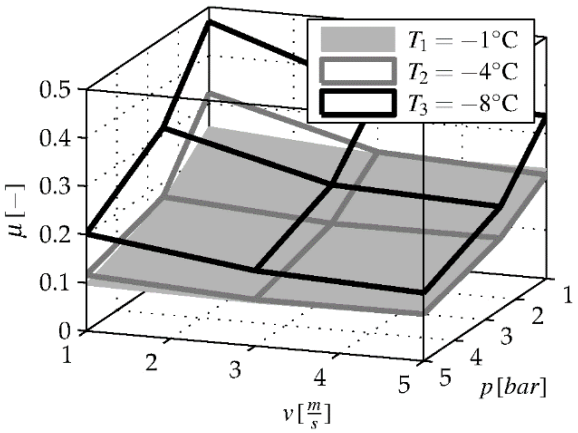

Graphic 5. - Test under snow

Through this test is obtained the frictional coefficient under snow. Moreover as it explained bellow the distance that the sample go through the snow can be measured with the linear potentiometer.

These results are demanded for companies such as Continental or Airbus.

3.3.- Theory Concepts

3.3.1.- Force transducer.

The 3-component force sensor is used for the dynamic and quasistatic measurement of the three orthogonal components of any force acting on the sensor (Fx, Fy and Fz).
3-component force sensors measure:

- Cutting forces during machining
- Impact forces in crash tests
- Recoil forces of rocket engines
- Vibration forces of components for space travel
- Friction forces
- Forces in product testing
- Ground reaction forces in biomechanics
- Vehicle forces on a road and a test stand
- Forces on a wind tunnel balance

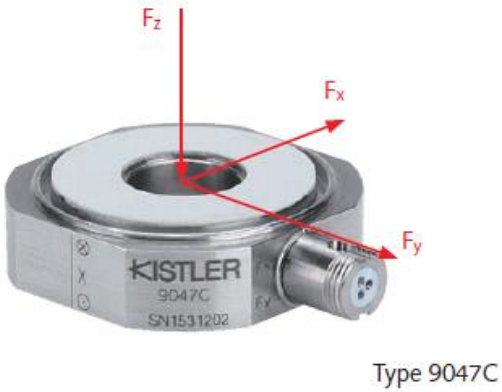

Image 3. - Force transducer

Quartz force sensor for measuring the three orthogonal components of a dynamic or quasistatic force acting in an arbitrary direction.

The sensor case contains three closely packed quartz rings mounted between two steel plates. Each quartz ring is sensitive to a force component. In accordance with the piezoelectric principle, the force produces a proportional electric charge. This is conducted via an electrode to the appropriate connector.
The two contact surfaces of the sensor are covered with ceramic layers, thereby allowing ground-insulated mounting in the machine structure.
The simple and vibration-resistant design of the sensor is very rigid resulting in a high natural frequency, which is a requirement for highly dynamic force measurements.
The three-pole connector V3 neg. (design protected) is provided with a positioning aid. This guarantees accurate assignment and centering of the connector pins and sockets before connection.
The plug connection is protected against rotation.
Quartz 3-component force sensors allow simple, direct and very precise measurements.
Manufacturing and tolerances.

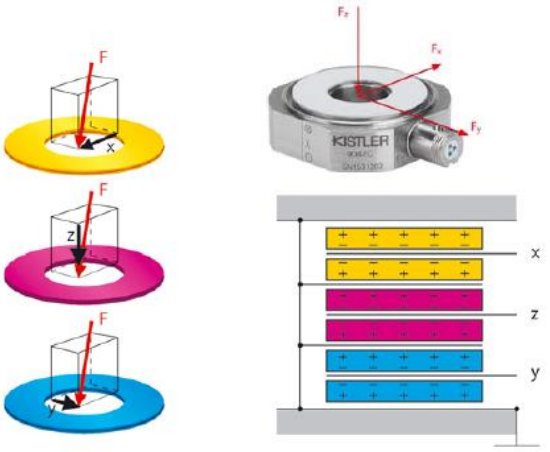

Image 4. - Force transducer operation

Positive or negative charges occur at the connections depending on the direction of the force. Negative charges produce positive voltages at the output of the charge amplifier and vice versa.

Mounting

The force sensor must be mounted under preload. The shear forces Fx and Fy are transferred by friction from the base and cover plates to the surface of the sensor.

To apply this preload it is necessary pretensioning elements.
A set of pretensioning elements consists of a pretensioning bolt (high-strength, stainless tool steel), a centering sleeve, an anti-friction washer and a nut.

Multicomponent and single-component force sensors have to be mounted under pretension to allow the shear forces Fx and Fy to be transferred by static friction from the base and cover plates

to the surfaces of the force sensor. The necessary pretension depends on the magnitude of the shear forces to be transferred.

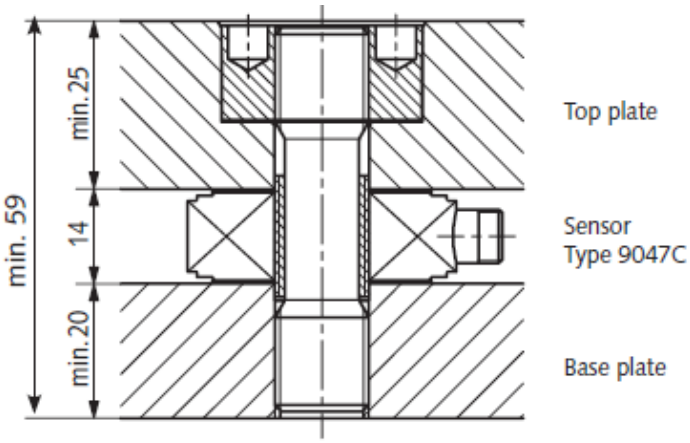

Image 5. - Mounting force transducer

3.3.2.- Von Mises yield criterion

The Von Mises yield criterion suggests that the yielding of materials begins when the second deviatoric stress invariant J_2 reaches a critical value. It is part of a plasticity theory that applies best to ductile materials, such as metals. Prior to yield, material response can be assumed to be anything i.e. nonlinear elastic, viscoelastic or simply linear elastic.

In materials science and engineering the Von Mises yield criterion can be also formulated in terms of the Von Mises stress or equivalent tensile stress,σ_v, a scalar stress value that can be computed from the Cauchy stress tensor. In this case, a material is said to start yielding when its Von Mises stress reaches a critical value known as the yield strength σ_y.

The Von Mises stress is used to predict yielding of materials under any loading condition from results of simple uniaxial tensile tests. The Von Mises stress satisfies the property that two stress states with equal distortion energy have equal Von Mises stress.

Because the Von Mises yield criterion is independent of the first stress invariant, I_1, it is applicable for the analysis of plastic deformation for ductile materials such as metals, as the onset of yield for these materials does not depend on the hydrostatic component of the stress tensor.

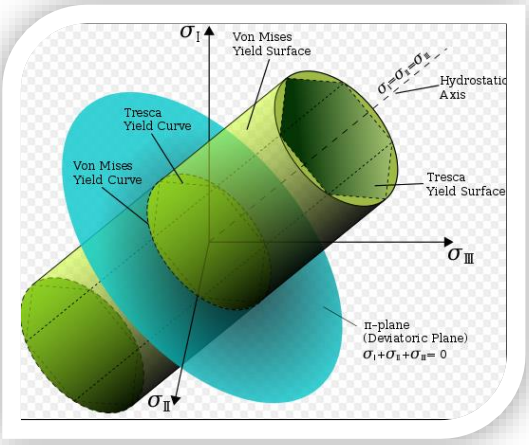

Image 6. - Von Mises yield criterion

Reduced von Mises equation for different stress conditions

Load scenario	Restrictions	Simplified von Mises equation
General	No restrictions	$\sigma_v = \sqrt{\frac{1}{2}[(\sigma_{11} - \sigma_{22})^2 + (\sigma_{22} - \sigma_{33})^2 + (\sigma_{33} - \sigma_{11})^2 + 6(\sigma_{12}^2 + \sigma_{23}^2 + \sigma_{31}^2)]}$
Principal stresses	No restrictions	$\sigma_v = \sqrt{\frac{1}{2}[(\sigma_1 - \sigma_2)^2 + (\sigma_2 - \sigma_3)^2 + (\sigma_3 - \sigma_1)^2]}$

Image 7. - Simplified Von Mises equation

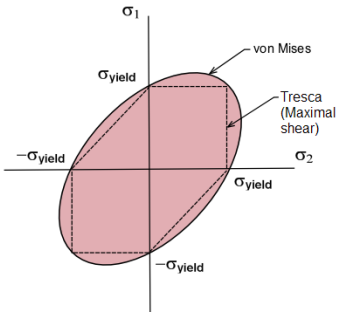

Image 8. - Intersection of the Von Mises yield criterion with the plane.

3.3.1.- Bearings

The bearings are a type of axle or bearing support that use small rolling elements to reduce friction between the rotating surfaces, since the rolling friction resistance is less than the frictional resistance due to slippage.

The advantages of using the bearings in place of friction bearings son:

Less friction in transient processes

They have the capacity to support combined axial and radial loads.

Require less axial space.

Lubrication is simpler and can work at higher temperatures without requiring rigorous maintenance.
Fundamentally they are standardized and easy to select elements.

The basic principle of running a bearing, light on reducing the magnitude of the frictional force with the base of the surface, introducing the small rolling elements, consequently the frictional force opposite the movement is much less.
Introduce the bearings to facilitate movement between the elements in contact with the rolling characteristics of these.
There are different types of bearings, but the following groups can be distinguished according to the geometry of the rolling elements:

- Ball bearing

Image 9. - Ball bearing

- Roller bearing
  - Cylindrical
  - Conics
  - Spherical
  - Needles

Image 10. - Roller bearing

Mounting tolerances and operating clearance

The theoretically possible operating clearance for the individual series is shown in the following tables and *Figure 1*.

Operating clearance for KH, KN..-B, KNO..-B

Mounting tolerance		Operating clearance All sizes	
Shaft	Bore		
h6	H7, K7	Normal operating clearance	Steel/ aluminium

Image 11. - Mounting tolerances

All the tolerances have been done with manufacture's restrictions as it has been shown in the table above.

Lubrication

Due to the initial greasing with a high quality grease and the integral lubricant reservoir, the linear bearings are maintenance-free for many applications; if necessary, however, they can be relubricated.

Linear ball bearings can be lubricated, depending on the design, via the openings in the outer ring or radial holes arranged in the center of the bearing.

In the units, lubrication is carried out via a separate lubrication nipple in the housing; location of the bearing in the housing and the relubrication devices are thus separate from each other

Operation temperatures

The bearings and housings can be used at operating temperatures from –30 °C to +80 °C

CHAPTER 4: New design and description of the technical solutions.

CHAPTER 4: New design and description of the technical solutions.

4.1.- Justification

In order to solve the problems previously cataloged, it was necessary to make a series of modifications that are described next.

INVENTOR has been used as a 3D software. It is allows the automation of the production of designs and drawings of mechanical parts, facilitating the design and drawing stages of the same.

Of the multiple work modules that INVENTOR offers we have used the following:

• Part Design: for the mechanical design of 3D parts.
• Assembly Design: for the assembly of the pieces previously created and the creation of the correct restrictions that allow to place each piece in the correct place.

It has also been used the FEM software, ANSYS WORKBENCH, which consists of a set of utilities that assist the engineer in the different phases that lead to the calculation and simulations of the new design.

4.2.- Description of the technical solutions.

The design of the different parts of carriage is shown below:

4.2.1.- To increase the normal force (2000 N)

To achieve this goal it was necessary to introduce two different bellows cylinder to get a range of loads between 100-2000 N. After looking in the market the final decision was introduce two bellow cylinder (ADVENTICS) due to the fact that they are the best which fit in the restrictions, as it has been shown in the next graphic.

Fig. 2

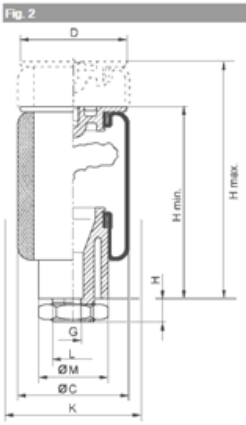

Part No.	Compressed air connection G	H min. [mm]	H max. [mm]	C [mm]	D [mm]	L	Ø M [mm]	K [mm]
0822419120	G 3/8	95	195	80	76,5	M30x1,5	50	100
0822419121	G 3/8	95	190	97	86,5	M30x1,5	60,5	115
0822419122	G 3/8	95	180	123	106,5	M30x1,5	81	140
0822419123	G 3/8	95	180	151	126,5	M30x1,5	89	170
0822419124	G 3/8	95	185	173	147,9	M30x1,5	114	190

Table 1. - Bellow cylinder specifications

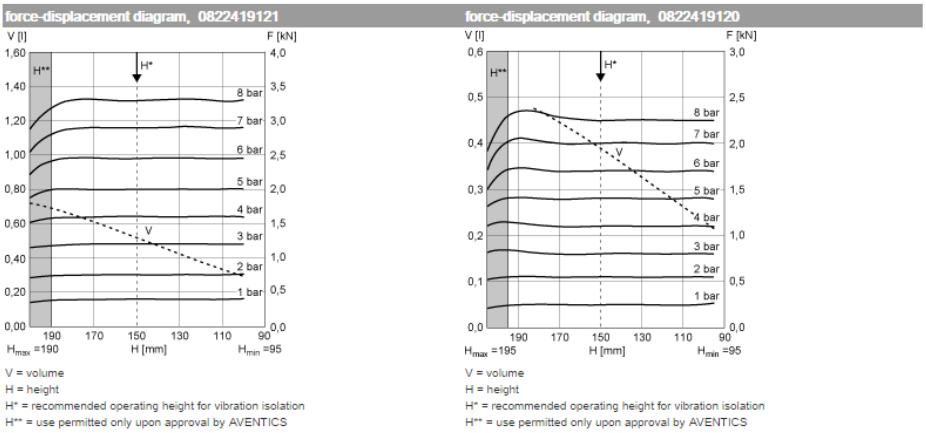

Graphic 6. - Force-displacement diagram bellow cylinder

As it can be observed in the above graphic the main advantage is that the load is uniform with the pressure. With the small bellow cylinder the load of 100 N with 1 bar can be achieved and with the big cylinder the maximum load of 2000 N is achieved.

Moreover, the load of 2000 N has to be achieved with a maximum of 6 bar, due to the fact that it is the restriction of the compressed air circuit.
The main task once the two bellow cylinder has been chosen is design a new frame for make it possible and how to fix it to the chassis and top frame.

4.2.2.- To design a new frame to take out the bellow cylinder.

Once the bellow cylinder was chosen, the next step was adapt the whole frame to make it possible. The big challenge in this new design was make the front frame in order to give the possibility of easily exchange the two bellows cylinders. It was

achieved with a wide open design and parts that can slide over each other.

In the following images it is shown the new design of the whole carriage.

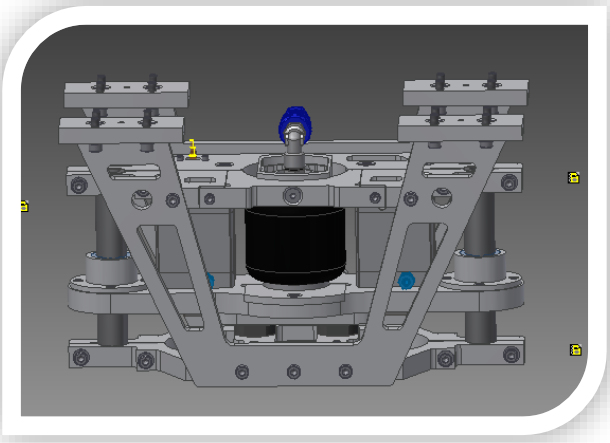

Image 12. - Front view of the carriage

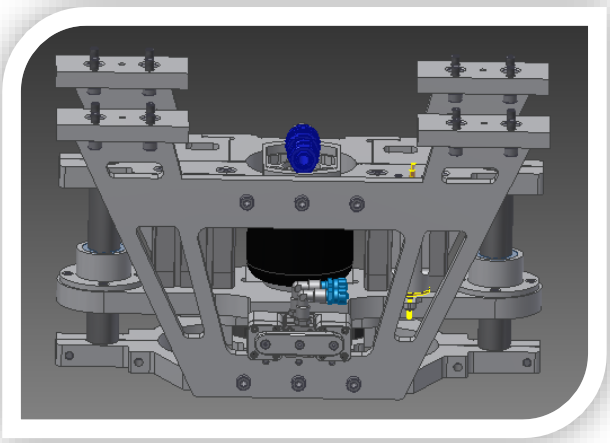

Image 13. - Back view of the carriage

This new design is lighter and easier to remove.
In the following blocks it is described the design process.

4.2.2.1.- Bottom and top frame

The bottom frame consist in two parts connected through bolts. This bottom frame is fixed.

The top frame has an innovative design easy to remove. The main item of the actual design is that it has a lot of screw connection, so for take out the bellow cylinder it is needed to unscrew all the structure.
This new design of the frame is explained in the following pictures:

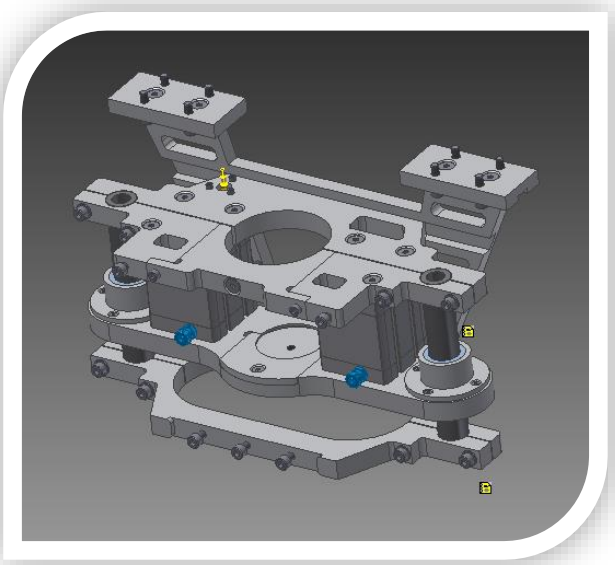

Image 14. - Bottom and top frame

As it has been shown above, this new desgin consist in three parts.

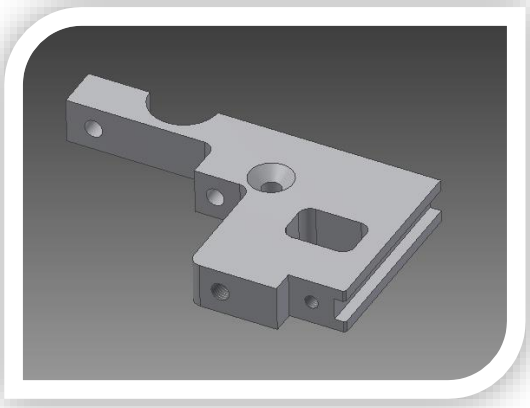

Image 15. - Top frame 1

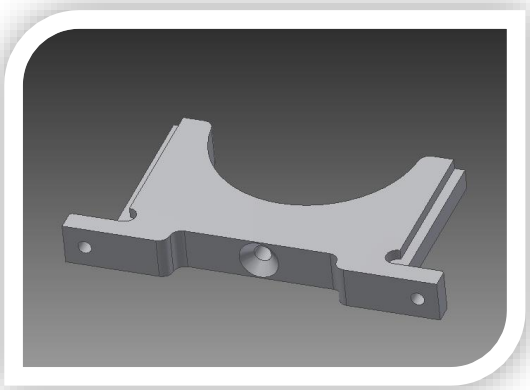

Image 16. - Top frame 3

With this new design only two screws are needed to connect these three parts. This is achieved with parts that can slide over

each other. Moreover, vertical and horizontal movements are fixed.
In addtion, this design has been made with the manufacturing restrictions.

Once the new design of the top frame has been made it, the next goal was design a new front frame as it is explained in the next block.

4.2.2.2.- Front and back frame

As it is shown in the following pictures, this part has been designed for take out the bellow cylinder without unscrew this front frame.
The front frame is connected with the bottom frame through 3 bolts and 2 more screws with the top frame.
With these bolts the position is fixed. In addition, to fix the vertical and horizontal movement it has a new design which allows to slide this front frame to the bottom frame.

In addition, as it is shown in the next picture, the design has been made with the manufacturing restrictions.

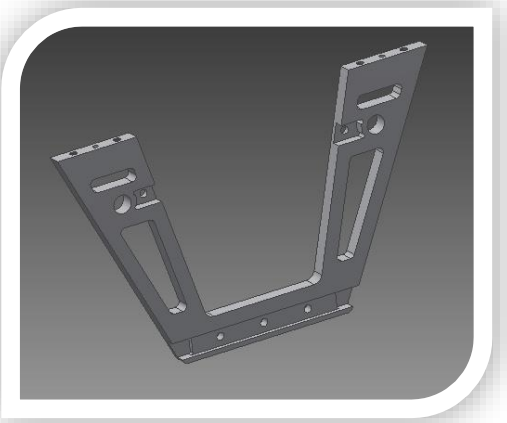

Image 17. - Front frame

It has a dimensional and geometric tolerances in the area where is going to be fixed with the bottom frame part. These tolerances are explained in the calculation's chapter.

In the following image, the back frame is shown.

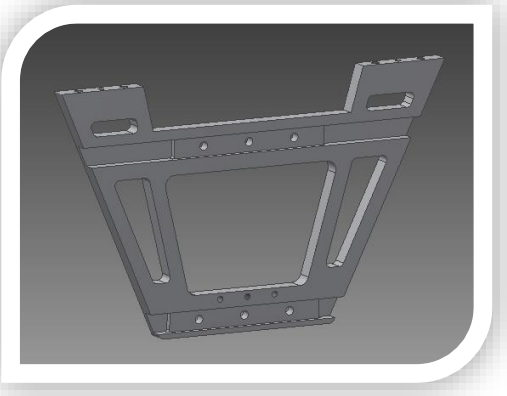

Image 18. - Back frame

The next step was to fix the bellow cylinder in vertical movement once the load is applied.

4.2.2.3.- Clamp between bellow cylinder with the top frame and chassis.

In the following images it is shown the part that fix the bellow cylinder with the top frame.

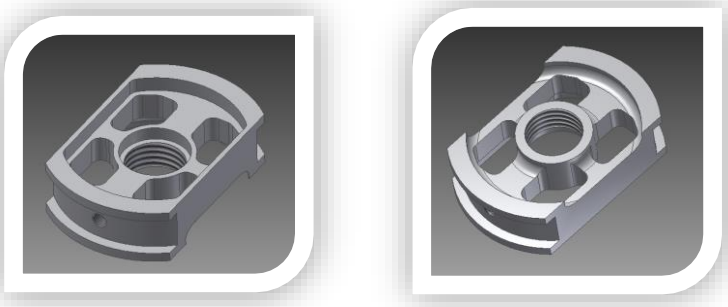

Image 19. - Clamp between bellow cylinder with the top frame

As it is shown in the above picture the vertical movement is fixed with this new part. It is screwed to the bellow cylinder.
The vertical movement is fix with this two edges which conntact up and down with the part showed before. Moreover it has a screw for fix the postion with the top frame, so it won't be able to move in any direction.

Firstly, the new design of the chassis is shown.

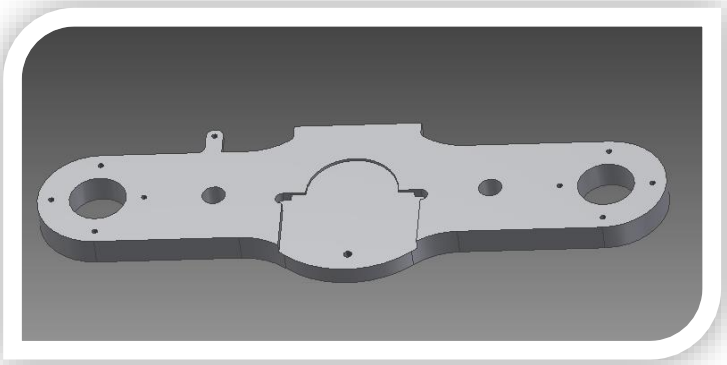

Image 20. - Chassis front view

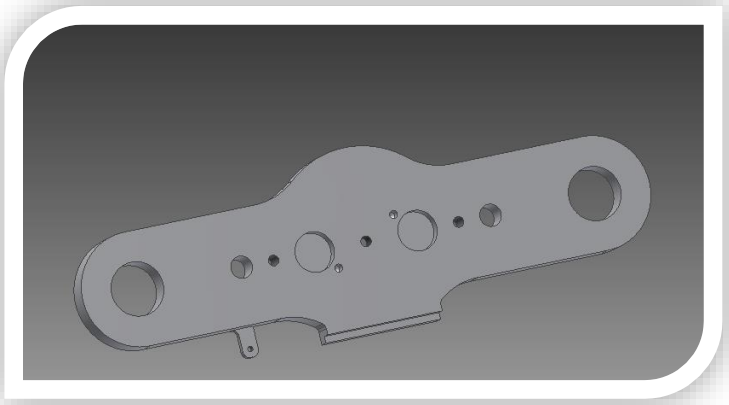

Image 21. - Chassis back view

It is lighter, really important for acceleration issue. Moreover, it is symetic and the load is applied in the center. This characteristic is a big advantage in order to not have a momentum.

In the following images it is explained how to fix the bellow cylinder to the chassis.

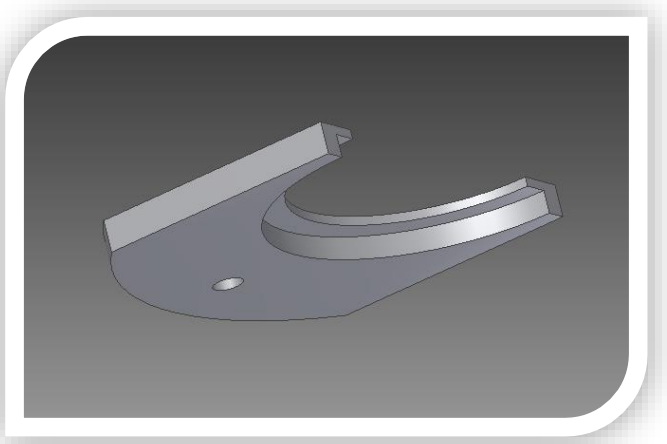

Image 22. - Clamp between bellow cylinder with chassis

As it is shown the movement has been fixed with this new part which slides once the bellow cylinder is in his position. This clamp allows to fix the position and the design of the chassis fix the vertical movement.
With these designs the bellow cylinder has been fixed.

4.2.2.1.- To design the connection (foot) between the base plate and the whole frame.

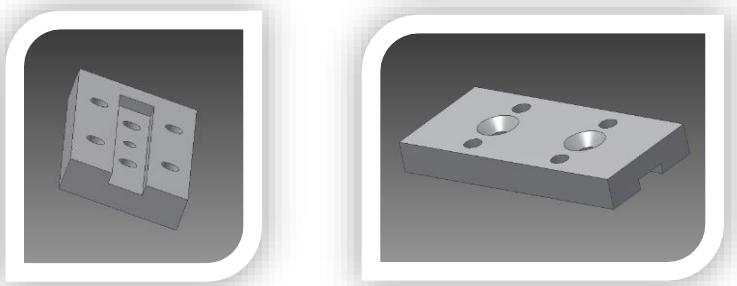

Image 23. - Foot

This part is necessary to fix the carriage with the actuator line or tooth belt which is going to be desgined in the next steps.
For this reason, the foot has been designed as it is shown in the above image. The foot slide into the front and back frame in order to fix the horizontal movement. The vertical movement is fixed through one pin which fix the positin and two bolts. These 2 bolts are DIN 7991 due to the fact that the head has to be inside for the connection with the railway. Moreover this screws fix better the horizontal movement.
The connection with the railway is through 4 x 4 = 16 bolts M8.
All the screw connections has been desgin to have the highest number of the same types of screws, which facilitate the work.

These feet will be fixed with the base plate.
In the following image a base plate to connect the carriage with the actuator line is shown.
It could be redisigned since it is neccesary to decide between actuator line or tooth belt.

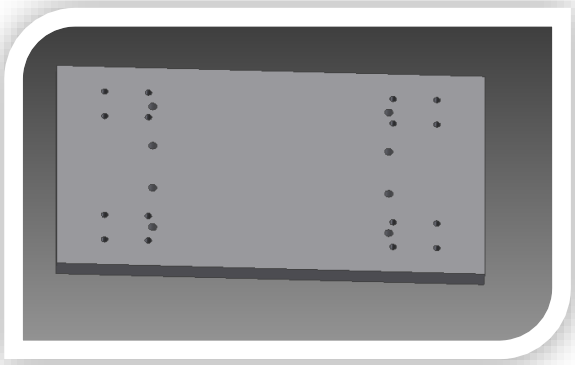

Image 24. - Base plate

Finally it is described the movement of the chassis through 2 hollow shaft and 2 Linear ball bearing showed in the next image:

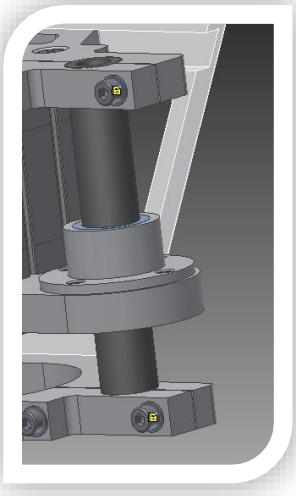

Image 25. - Movement of the chassis

4.2.3.- New design to pull up the chassis.

This new design consists in introduce two pistons in a symmetric position.

The main goal was decide which piston was needed due to with the actual design, the piston doesn't have the necessary force to pull up the chassis when the pressure of 5 bar is applied. In order to solve this problem, it is necessary to descend the pressure to 1 bar to take back the carriage.

This is a big problem due to sometimes this process is forgotten and the carriage hits the path in his way back, consequently the test is wrong.

The solution was introduce two pistons due to the fact that one of the goals at the beginning was make a symmetric design.

The design and the main specifications of this piston are shown in the following pictures. All the characteristics of the piston are shown in the Annexes.

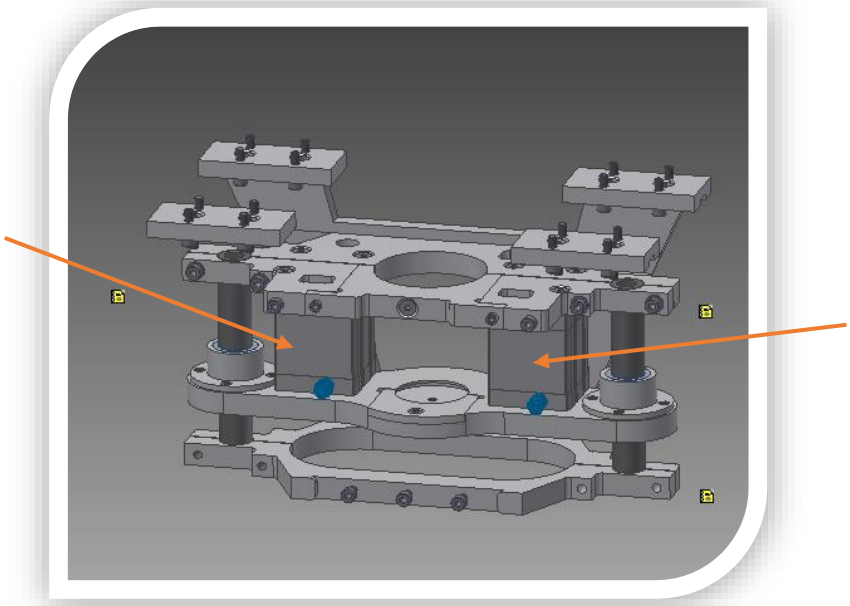

Image 26. - New design to pull up the chassis.

Main characteristics of the piston:

- Stroke: 40 mm
- Theoretical force at 6 bar, return stroke: 1750 N

The whole return force is 1750 N x 2 = 3500 N
The stroke of 40 mm is neccesary, due to the fact that the maximum stroke of the chasis is 35 mm.
This 5mm are needed because when the piston has the advanced stroke it has to go further and realease the chassis. As it is shown in the picture, the piston is double acting. However we only introduce pressure air to pull up the chassis, due to the fact that the advance stroke is not necessary. When the bellow cylinder applies the load, the piston realises without force.

Once the piston had been chosen, the next step was design the connection with the chasis for pulling it up.
For this reason a screw with a normal head that make it easy to unscrew was designed.

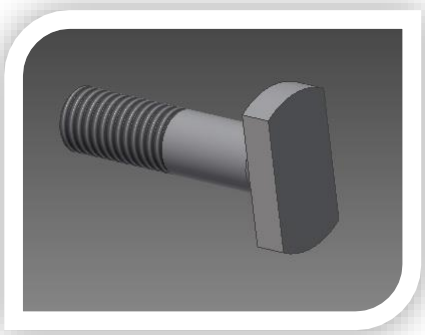

Image 27. - Bolt's piston

4.2.4.- To design a new mechanical design to support the chassis under the maximum load.

This new system has a small piston which transmits the stroke to two bolts. These bolts are supported through two linear ball bearing which support the load. The next images show the final assembly.

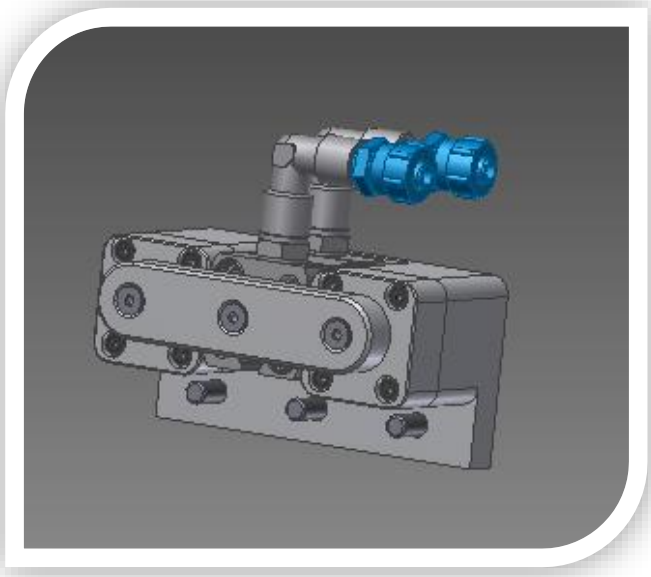

Image 28. - New system to support the chassis under the maximum load.

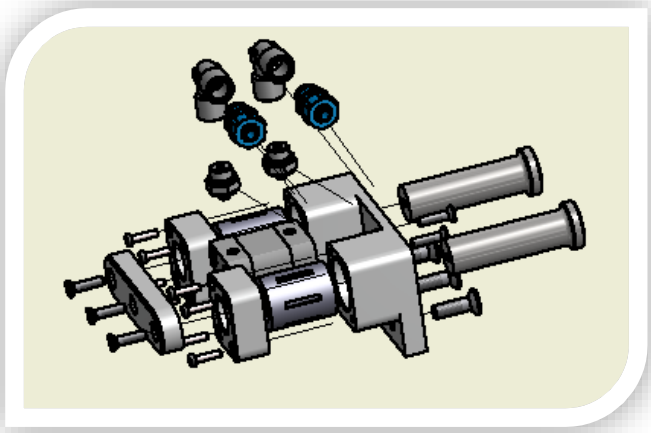

Image 29. - Explosion of the new design

This system is necessary in order to apply the normal load of 2000 N only in convenient time.
This system has the following parts. The specifications of each part are at the end of this project (Annexes)

- Piston:
- Stroke: 5 mm

It transmits the stroke of 5 mm due to the fact that the shaft is too weak to support the load of 2000 N.
To support this load two linear ball bearing were introduced. The main characteristic is shown below. The specifications are shown at the end of this project (Annexes)

- *Linear ball bearing KH16-PP*
- Basic dynamic load rating: $C_{max} = 1060\ N$

Due to the fact that there are two linear ball bearings:

$$1060 \times 2 = 2120\ N$$

Moreover to test this bolt one FEA test has been made as it will be shown in the simulation's chapter.

4.2.5.- To introduce a linear potentiometer.

It is necessary when tests under snow are done in order to measure the distance that the sample can be introduced into the snow. The brand of this linear transducer is WAYCON due to the fact that it was the best to achieve all the specifications.

The main characteristic are described next. For further details go to the end of this project (ANEXO)

- Stroke=50 mm
- Max Displacement speed movement = 10 m/s

Once the linear potentiometer was selected, the next step was design a cover to join it with the rest of the carriage.
The following cover plastic part connects it with the top frame:

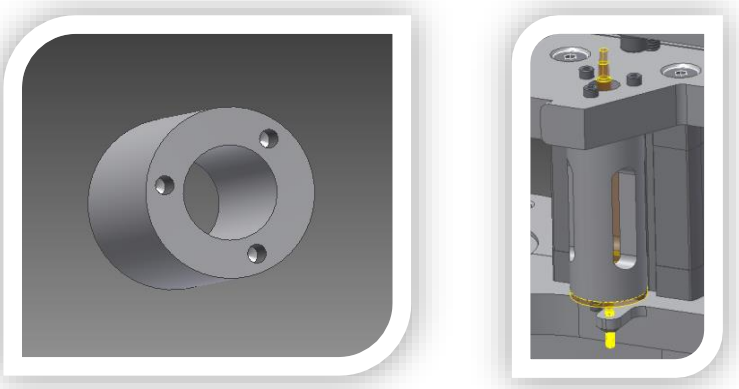

Image 30. - Linear potentiometer's cover

4.2.6.- New design of the sample holder.

The goal was make a new design in order to make it easier to remove. To achieve this goal one new part was designed which is screw to the sample holder as it is shown in the next image.

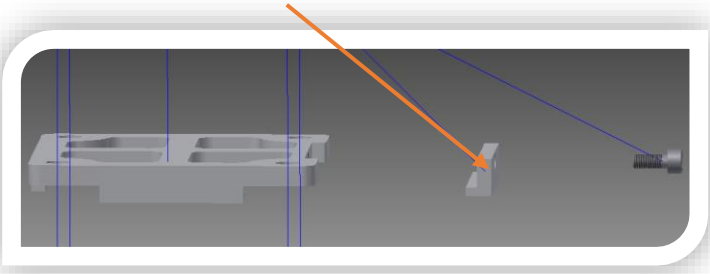

Image 31. - New part of the simple holder

Finally, all the connections that involved compressed air were designed according to security terms.
In the next image the bellow cylinder connections are shown.

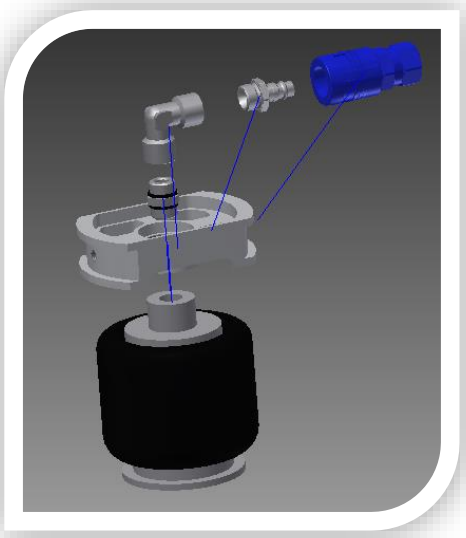

Image 32. - Compressed air connections

This design allows to join the pipe easily. Moreover it is secure if the pipe is unscrewed.

CHAPTER 5: Calculations and simulations

CHAPTER 5: Calculations and simulations

5.1. Calculations

5.1.1. Bolts

3 ways of failures:

- Gapping
- Slippage
- Bolt strength

NOMENCLATURE:

Pnom: nominal Preload (N)
Fmax: Max load due to the bolt's tensile stress (N)
Fall: permissible tensile load (N)
n: Coefficient without load (usually: 0.5)
k: Coefficient of stiffness ratio of the joint (frequent value: 0.16)
η: Coefficient of friction
N: Number of bolts in the union
Qmax: Maximum load due to shear stress on bolt (N)
Qall: Permissible shear load (N)
As: Bolt cross-sectional area (m^2)
K1: Coefficient (frequent value: 0.65)

5.1.1.1. Gapping

Equation 1: Maximum load due to tensile stress at the joint- Gapping

$$F_{max} = F_t \cdot [1 - n \cdot k]$$

F_t: Maximum tensile load acting on the bolt (analysis result) F_t=2000 N

$$F_{max} = 2000 \cdot [1 - 0.5 \cdot 0.16] = 1840\ N$$

Applying a safety factor of 1.2

$$\boldsymbol{F_{max}} = 1840\ N \cdot 1.2 = \mathbf{2208\ N}$$

Equation 2: Permisible Load- Gapping

$$\boldsymbol{F_{all}} = \mathbf{0.85} \cdot \boldsymbol{P_{nom}}$$

Equation 3: Nominal preload on a bolt- Gapping

$$\boldsymbol{P_{nom}} = \boldsymbol{S_y} \cdot \boldsymbol{A_s} \cdot \boldsymbol{K1}$$

Knowing that K1 = 0.65 and that the creep limit (varies depending on the quality of the bolt, the allowable load is calculated for each of the metrics and for all grades).
Finally, the results are shown in the following table:

D(mm)	As(mm)	Fall(N) [4.6]	Fall(N) [4.8]	Fall(N) [5.8]	Fall(N) [8.8]	Fall(N) [9.8]	Fall(N) [10.9]	Fall(N) [12.9]
1,6	1,07	141,882	200,9995	248,2935	390,1755	425,646	555,7045	650,2925
2	1,79	237,354	336,2515	415,3695	652,7235	712,062	929,6365	1087,8725
2,5	2,98	395,148	559,793	691,509	1086,657	1185,444	1547,663	1811,095
3	4,47	592,722	839,6895	1037,2635	1629,9855	1778,166	2321,4945	2716,6425
3,5	6	795,6	1127,1	1392,3	2187,9	2386,8	3116,1	3646,5
4	7,75	1027,65	1455,8375	1798,3875	2826,0375	3082,95	4024,9625	4710,0625
5	12,7	1684,02	2385,695	2947,035	4631,055	5052,06	6595,745	7718,425
6	17,9	2373,54	3362,515	4153,695	6527,235	7120,62	9296,365	10878,725
8	32,8	4349,28	6161,48	7611,24	11960,52	13047,84	17034,68	19934,2
10	52,3	6934,98	9824,555	12136,215	19071,195	20804,94	27162,005	31785,325
12	76,3	10117,38	14332,955	17705,415	27822,795	30352,14	39626,405	46371,325
14	104	13790,4	19536,4	24133,2	37923,6	41371,2	54012,4	63206
16	144	19094,4	27050,4	33415,2	52509,6	57283,2	74786,4	87516
20	225	29835	42266,25	52211,25	82046,25	89505	116853,75	136743,75
24	324	42962,4	60863,4	75184,2	118146,6	128887,2	168269,4	196911
30	519	68819,4	97494,15	120433,95	189253,35	206458,2	269542,65	315422,25
36	759	100643,4	142578,15	176125,95	276769,35	301930,2	394186,65	461282,25
42	1050	139230	197242,5	243652,5	382882,5	417690	545317,5	638137,5
48	1380	182988	259233	320229	503217	548964	716703	838695
56	1910	253266	358793,5	443215,5	696481,5	759798	991958,5	1160802,5
64	2520	334152	473382	584766	918918	1002456	1308762	1531530
72	3280	434928	616148	761124	1196052	1304784	1703468	1993420
80	4140	548964	777699	960687	1509651	1646892	2150109	2516085
90	5360	710736	1006876	1243788	1954524	2132208	2783716	3257540
100	6740	893724	1266109	1564017	2457741	2681172	3500419	4096235

Table 2. - Permisible Load (F_{all}), Gapping

In view of the results, we can conclude that for nominal diameters bigger than or equal to M4 (quality 8.8) it is satisfied that the permissible load on the bolt is bigger than the Maximum Load due to the tensile stress at the joint for all grades, so no gapping occurs.

5.1.1.2. Slippage

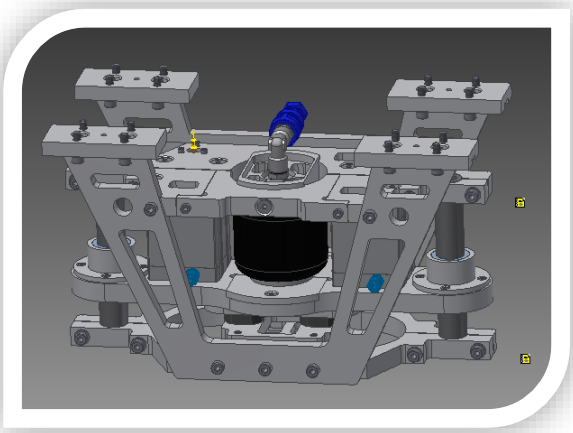

Image 33. - Slippage

Equation 4: Maximum load due to tensile stress at the joint- Slippage

$$\boldsymbol{Q_{max} = mod|F_x + F_y| = \sqrt{{F_x}^2 + {F_y}^2} = \sqrt{6000^2 + 2000^2}}$$

$$Q_{max} = 6325N$$

Applying a safety factor of 1.2

$$Q_{max} = 6325N * 1.2 = 7590\ N$$

Equation 5: Permissible Load- Slippage

$$Q_{all} = 0.85 \cdot P_{nom} \cdot n \cdot N$$

$$P_{nom} = S_y \cdot A_s \cdot K1$$

We have taken a coefficient of friction n = 0.4 since it is the most unfavorable and taking into account that the contact is metal-metal.

From this formula we have calculated the permissible load of each of the bolts and their qualities

D(mm)	As(mm)	Qall(N) [4.6]	Qall(N) [4.8]	Qall(N) [5.8]	Qall(N) [8.8]	Qall(N) [9.8]	Qall(N) [10.9]	Qall(N) [12.9]
1,6	1,07	1702,584	2411,994	2979,522	4682,106	5107,752	6668,454	7803,51
2	1,79	2848,248	4035,018	4984,434	7832,682	8544,744	11155,638	13054,47
2,5	2,98	4741,776	6717,516	8298,108	13039,884	14225,328	18571,956	21733,14
3	4,47	7112,664	10076,274	12447,162	19559,826	21337,992	27857,934	32599,71
3,5	6	9547,2	13525,2	16707,6	26254,8	28641,6	37393,2	43758
4	7,75	12331,8	17470,05	21580,65	33912,45	36995,4	48299,55	56520,75
5	12,7	20208,24	28628,34	35364,42	55572,66	60624,72	79148,94	92621,1
6	17,9	28482,48	40350,18	49844,34	78326,82	85447,44	111556,38	130544,7
8	32,8	52191,36	73937,76	91334,88	143526,24	156574,08	204416,16	239210,4
10	52,3	83219,76	117894,66	145634,58	228854,34	249659,28	325944,06	381423,9
12	76,3	121408,56	171995,46	212464,98	333873,54	364225,68	475516,86	556455,9
14	104	165484,8	234436,8	289598,4	455083,2	496454,4	648148,8	758472
16	144	229132,8	324604,8	400982,4	630115,2	687398,4	897436,8	1050192
20	225	358020	507195	626535	984555	1074060	1402245	1640925
24	324	515548,8	730360,8	902210,4	1417759,2	1546646,4	2019232,8	2362932
30	519	825832,8	1169929,8	1445207,4	2271040,2	2477498,4	3234511,8	3785067
36	759	1207720,8	1710937,8	2113511,4	3321232,2	3623162,4	4730239,8	5535387
42	1050	1670760	2366910	2923830	4594590	5012280	6543810	7657650
48	1380	2195856	3110796	3842748	6038604	6587568	8600436	10064340
56	1910	3039192	4305522	5318586	8357778	9117576	11903502	13929630
64	2520	4009824	5680584	7017192	11027016	12029472	15705144	18378360
72	3280	5219136	7393776	9133488	14352624	15657408	20441616	23921040
80	4140	6587568	9332388	11528244	18115812	19762704	25801308	30193020
90	5360	8528832	12082512	14925456	23454288	25586496	33404592	39090480
100	6740	10724688	15193308	18768204	29492892	32174064	42005028	49154820

Table 3. - Permissible Load (Q_{all}), Slippage

In view of the results, we can conclude that slippage is not a problem in this case.

5.1.1.3. Bolt strength

Equation 6: Maximum load to tensile stress at the joint- Bolt strength

$$F_{max} = 1.15 \cdot P_{nom} + F_t \cdot k$$

$$F_{max} = 1.15 \cdot P_{nom} + 2000 \cdot 0.16$$

$$P_{nom} = S_y \cdot A_s \cdot K1$$

Equation 7: Permissible Load- Bolt strenght

$$F_{all} = S_y \cdot A_s$$

The following table shows the comparison between loads for each of the nominal diameters:

D(mm)	As(mm)	Fall(N) [4.6]	Fall(N) [4.8]	Fall(N) [5.8]	Fall(N) [8.8]	Fall(N) [9.8]	Fall(N) [10.9]	Fall(N) [12.9]
1,6	1,07	256,8	363,8	449,4	706,2	770,4	1005,8	1177
2	1,79	429,6	608,6	751,8	1181,4	1288,8	1682,6	1969
2,5	2,98	715,2	1013,2	1251,6	1966,8	2145,6	2801,2	3278
3	4,47	1072,8	1519,8	1877,4	2950,2	3218,4	4201,8	4917
3,5	6	1440	2040	2520	3960	4320	5640	6600
4	7,75	1860	2635	3255	5115	5580	7285	8525
5	12,7	3048	4318	5334	8382	9144	11938	13970
6	17,9	4296	6086	7518	11814	12888	16826	19690
8	32,8	7872	11152	13776	21648	23616	30832	36080
10	52,3	12552	17782	21966	34518	37656	49162	57530
12	76,3	18312	25942	32046	50358	54936	71722	83930
14	104	24960	35360	43680	68640	74880	97760	114400
16	144	34560	48960	60480	95040	103680	135360	158400
20	225	54000	76500	94500	148500	162000	211500	247500
24	324	77760	110160	136080	213840	233280	304560	356400
30	519	124560	176460	217980	342540	373680	487860	570900
36	759	182160	258060	318780	500940	546480	713460	834900
42	1050	252000	357000	441000	693000	756000	987000	1155000
48	1380	331200	469200	579600	910800	993600	1297200	1518000
56	1910	458400	649400	802200	1260600	1375200	1795400	2101000
64	2520	604800	856800	1058400	1663200	1814400	2368800	2772000
72	3280	787200	1115200	1377600	2164800	2361600	3083200	3608000
80	4140	993600	1407600	1738800	2732400	2980800	3891600	4554000
90	5360	1286400	1822400	2251200	3537600	3859200	5038400	5896000
100	6740	1617600	2291600	2830800	4448400	4852800	6335600	7414000

D(mm)	As(mm)	Fmax(N) [4.6]	Fmax(N) [4.8]	Fmax(N) [5.8]	Fmax(N) [8.8]	Fmax(N) [9.8]	Fmax(N) [10.9]	Fmax(N) [12.9]
1,6	1,07	511,958	591,9405	655,9265	847,8845	895,874	1071,8355	1199,8075
2	1,79	641,126	774,9285	881,9705	1203,0965	1283,378	1577,7435	1791,8275
2,5	2,98	854,612	1077,367	1255,571	1790,183	1923,836	2413,897	2770,305
3	4,47	1121,918	1456,0505	1723,3565	2525,2745	2725,754	3460,8455	3995,4575
3,5	6	1396,4	1844,9	2203,7	3280,1	3549,2	4535,9	5253,5
4	7,75	1710,35	2289,6625	2753,1125	4143,4625	4491,05	5765,5375	6692,4375
5	12,7	2598,38	3547,705	4307,165	6585,545	7155,14	9243,655	10762,575
6	17,9	3531,26	4869,285	5939,705	9150,965	9953,78	12897,435	15038,275
8	32,8	6204,32	8656,12	10617,56	16501,88	17972,96	23366,92	27289,8
10	52,3	9702,62	13612,045	16739,585	26122,205	28467,86	37068,595	43323,675
12	76,3	14008,22	19711,645	24274,385	37962,605	41384,66	53932,195	63057,675
14	104	18977,6	26751,6	32970,8	51628,4	56292,8	73395,6	85834
16	144	26153,6	36917,6	45528,8	71362,4	77820,8	101501,6	118724
20	225	40685	57503,75	70958,75	111323,75	121415	158416,25	185326,25
24	324	58445,6	82664,6	102039,8	160165,4	174696,8	227978,6	266729
30	519	93428,6	132223,85	163260,05	256368,65	279645,8	364995,35	427067,75
36	759	136484,6	193219,85	238608,05	374772,65	408813,8	533631,35	624407,75
42	1050	188690	267177,5	329967,5	518337,5	565430	738102,5	863682,5
48	1380	247892	351047	433571	681143	743036	969977	1135025
56	1910	342974	485746,5	599964,5	942618,5	1028282	1342381,5	1570817,5
64	2520	452408	640778	791474	1243562	1356584	1770998	2072390
72	3280	588752	833932	1030076	1618508	1765616	2305012	2697300
80	4140	743036	1052501	1300073	2042789	2228468	2909291	3404435
90	5360	961904	1362564	1683092	2644676	2885072	3766524	4407580
100	6740	1209476	1713291	2116343	3325499	3627788	4736181	5542285

Table 4. - Maximum and Permissible Load (F_{all} y F_{max}), Bolt Strength

In view of the results, we can conclude that for nominal diameters bigger than or equal to M4 (quality 8.8) it is satisfied that the permissible load on the bolt is bigger than the Maximum Load due to the tensile stress at the joint for all grades, so no bolt strength occurs.

Conclusion

Once the three criteria have been done, we conclude that the most restrictive condition for our case is that due to the gapping This result is consistent since the bolt have to support the normal load of 2000 N.

Taking into account these results, quality 8.8 (M4 M6 M8 M10) has been selected as it meets all of our restrictions. It is also the most widespread quality, therefore the most economical.

5.1.2. Linear Tolerances

5.1.2.1. Tolerance between Top frame 1-3-4

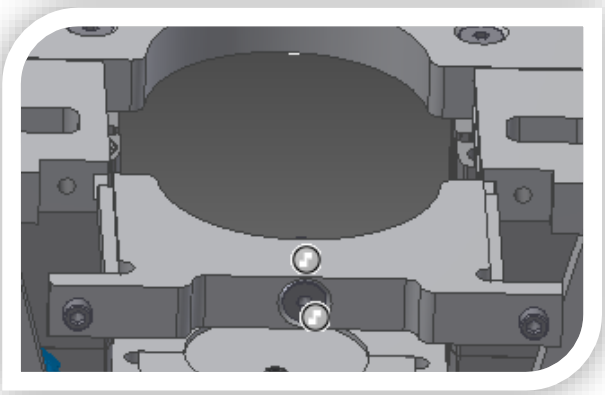

Image 34. - Tolerance between Top frame 1-3-4

The groove is manufactured in the base hole system. This slot has a play with the male between 30 and 130 μm.

Calculations.
T=Tolerance
P_{max}=Play max
P_{min}=Play min
D_{max}=Diameter max female (hole)
D_{min}= Diameter min female (hole)
d_{max}=diameter max male (shaft)
d_{min}= diameter min male (shaft)
F_{max}=Fix max
F_{min}=Fix min

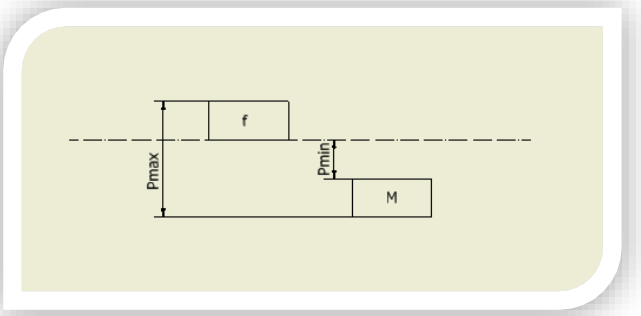

Image 35. - Play

$$P_{max} = 130\ \mu m$$
$$P_{min} = 30\ \mu m$$

Male	T=58 μm	IT10
Female	T=36 μm	IT9

$$T_t = 58 + 36 = 94 < P_{max} - P_{min}$$

Equation 8: Play maximum

$$\boldsymbol{P_{max} = D_{max} - d_{min}}$$

$$d_{min} = D_{max} - P_{max} = (10 + 0.058) - 0.13 = 9.928mm$$

Equation 9: Play minimum

$$\boldsymbol{P_{min} = D_{min} - d_{max}}$$

$$d_{Max} = D_{min} - P_{min} = 10 - 0.030 = 9.97mm$$

Once the maximum and minimum diameter is obtained is time to choose the tolerance and check it out.

$$\emptyset 10e9(-25/-61\ \mu m)$$

$$P_{max} = D_{max} - d_{min} = (10 + 0.058) - (10 - 0.061) = 0.119 < 130\ \mu m$$

$$P_{min} = D_{min} - d_{max} = 10 - (10 - 0.025) = 25 < 30\mu m$$

Solution

$$\emptyset \mathbf{10}\ \boldsymbol{H10/e9}$$

5.1.2.1. Tolerance between Front frame and bottom frame

Single shaft system with quality 9. Fix between:

$$F_{max} = 132\mu m$$
$$F_{min} = 8\mu m$$

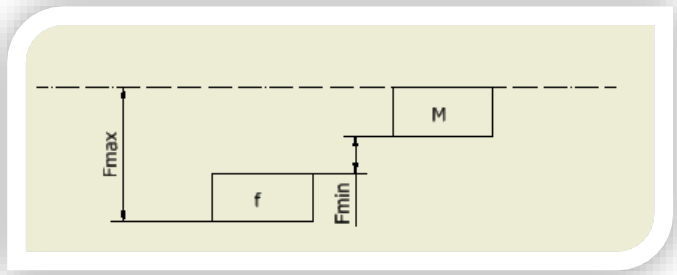

Image 36. - Fix

Equation 10: Fix maximum

$$\boldsymbol{F_{max} = d_{Max} - D_{min}}$$

$$D_{min} = d_{Max} - F_{max} = 165 - 0.132 = 164.868mm$$

Equation 11: Fix minimum

$$\boldsymbol{F_{min} = d_{min} - D_{max}}$$

$$D_{max} = d_{min} - F_{min} = (165 - 0.036) - 0.008 = 164.956mm$$

$$T = 88\mu m - IT8$$

Chose the tolerance and check it out.

$$\emptyset 165P8(-43/-106\mu m)$$

$$F_{max} = d_{Max} - D_{min} = 165 - (165 - 0.106) = 106 < 132\ \mu m$$

$$F_{min} = d_{min} - D_{max} = (165 - 0.036) - (165 - 0.043) = 7 < 8\mu m$$

Solution

$$\boldsymbol{\emptyset 165P8/h9}$$

5.1.3. X and Y force component in the carriage

Finally it has been calculated the component X and Y of the force. It is necessary to calculate this value in order to design the belt or the actuator line in future lines.

Mass of the carriage

The mass of the carriage is obtained once the simulations have been done. In the next table every mass is shown:

Name	Identifier	Units	Weight (kg)
Front frame	1101	1	1,07
Back frame	1102	1	1,35
Foot	1103	4	0,92
Bottom frame 1	1104	1	0,61
Bottom frame 2	1105	1	0,61
Top frame 1	1106	1	0,34
Top frame 2	1107	1	1,1
Top frame 3	1108	1	0,42
Top frame 4	1109	1	0,34
Chasis	1110	1	2,7
Clamp bearing	1111	1	0,1
Bottom Clamp bellow	1112	1	0,067
Screw piston	1113	2	0,074
Plastic cover	1114	1	1,35
Hollow shaft	KH30	2	0,2
Ball bearing	WH30	2	1,36
Piston	572705_ADN-63-40-I-PPS-A	2	1,44
Quick connector	2028_CK-1_8-PK-6	2	0,015
Linear potentiometer	LZW1-F-50	1	0,1
Clamp Holder	1202	1	0,109
Base plate	1203	1	0,305
Top plate	1204	1	0,27
Bolt	1205	2	0,1
Force transducer	Kistler 9047C	2	0,04
Bellow cylinder	822419121	1	0,5
Top Clamp bellow	1301	1	0,2
Double nipple E-3.8-3.8	3578_E-3_8-3_8	1	0,005
Elbow fitting	8030211_NPFC-L-2G38-F	1	0,01
Coupling plug	151780_KSS6-3_8-A	1	0,005
Quick coupling socket	531654_KDS6-CK-13	1	0,025
Shell	1401	1	0,145
Stock over	1402	2	0,027
Connector	1403	1	0,034
Bolt	1404	2	0,204
Piston	536226_ADN-16-5-I-P-A	1	0,08
Linear ball bearing	KH16-PP	2	0,03
Double nipple	4138_E-M5-1_8	2	0,005
Elbow fitting	8030209_NPFC-L-2G18-F	2	0,01
Quick connector	2028_CK-1_8-PK-6	2	0,005
Screws			1
TOTAL			17,275

Table 5. - Mass of the carriage

The X component of the force is calculated through the following formula:

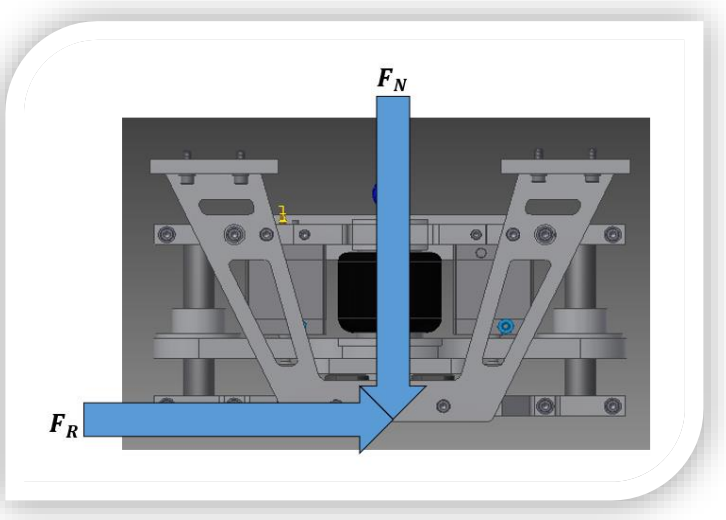

Image 37. - Force components applied in the carriage

Restrictions

- a=50 …100 m/s^2
- Vmax=10 m/s
- F_N=2000 N

Calculation:

Equation 12: Frictional force applied in the carriage

$$\boldsymbol{F_R = (F_N * \mu) + mass * acceleration}$$

$$F_R = 2000 \times 2 + 17.3 \times 100 = 5730\ N$$

$$F_R = 2000 \times 2 + 17.3 \times 50 = 4865\ N$$

5.2. Simulations

FEA. General procedure

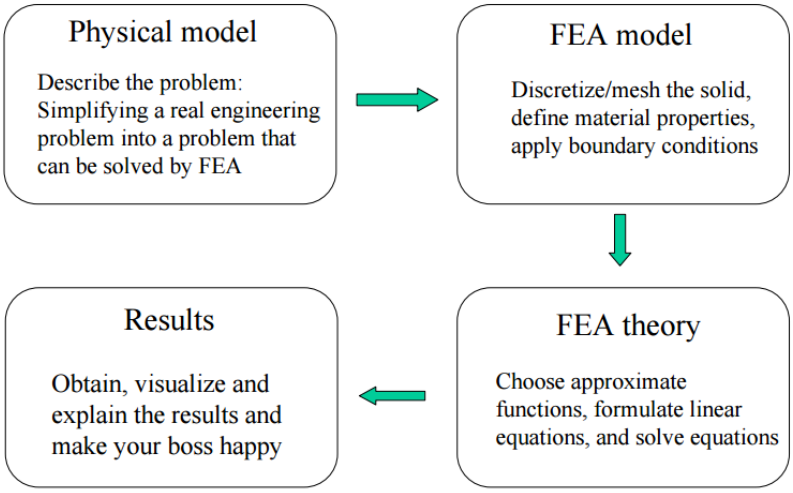

It is important to explain that these simulations help us to give an overview of the carriage's behavior with the maximum force. However the bearings which support the transversal load are not included.

In the next image it is explained the working diagram.

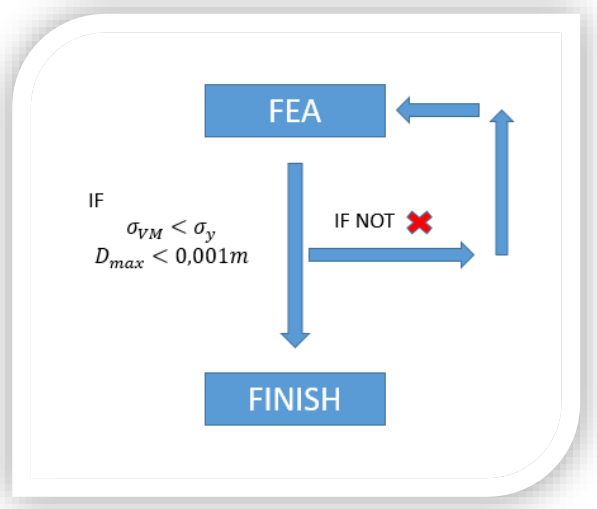

Image 38. - Flow chart of simulations

Data

Aluminum: σ_{YA} =0.280MPa
Stainless steel: σ_{YS} =280MPa
Front frame (aluminum)
Bolt (Stainless steel)

Front frame (aluminum)

Firstly, the front frame is simulated with all the material.

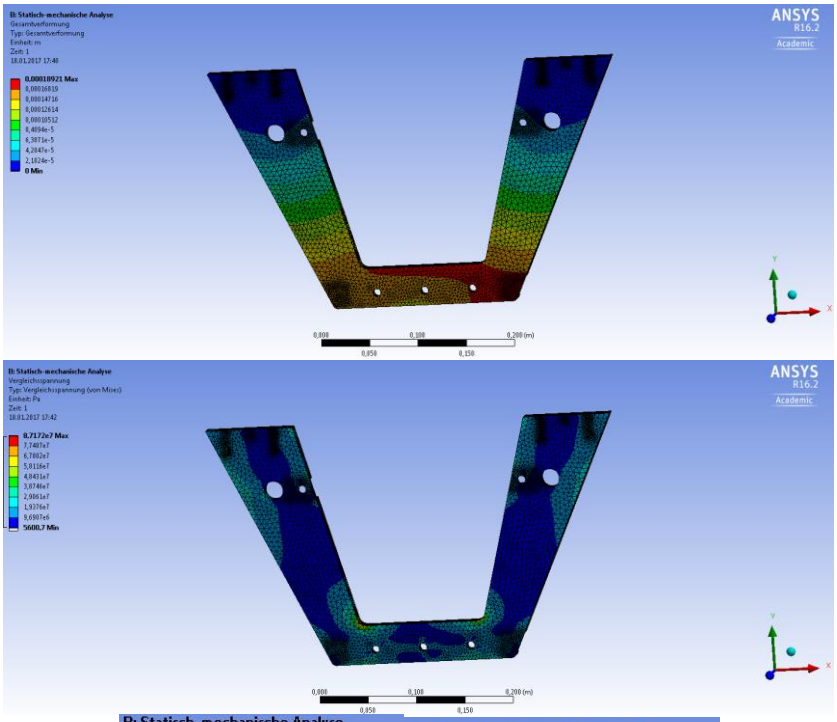

B: Statisch-mechanische Analyse
Gesamtverformung
Typ: Gesamtverformung
Einheit: m
Zeit: 1
18.01.2017 17:40
0,00018921 Max
0,00016819
0,00014716
0,00012614
0,00010512
8,4094e-5
6,3071e-5
4,2047e-5
2,1024e-5
0 Min
B: Statisch-mechanische Analyse
Vergleichsspannung
Typ: Vergleichsspannung (von Mises)
Einheit: Pa
Zeit: 1
18.01.2017 17:42
8,7172e7 Max
7,7487e7
6,7802e7
5,8116e7
4,8431e7
3,8746e7
2,9061e7
1,9376e7
9,6907e6
5600,7 Min

Image 39. - Simulation with all the material

The conclusion after this first simulation is that it is possible to reduce material. Moreover this is needed to satisfy the acceleration restriction.

Iteration 1

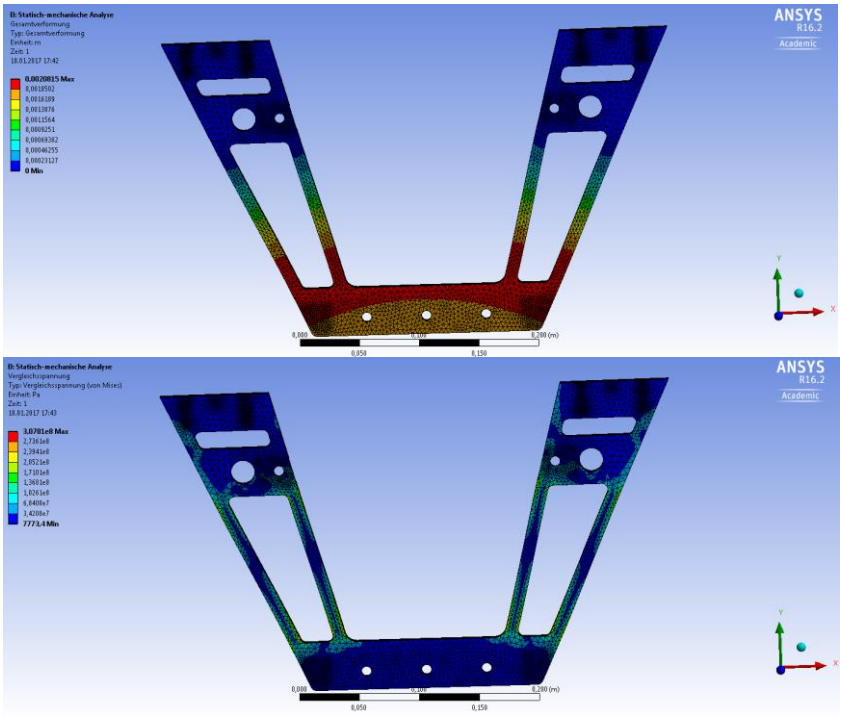

B: Statisch-mechanische Analyse
Gesamtverformung
Typ: Gesamtverformung
Einheit: m
Zeit: 1
18.01.2017 17:42
0,0020815 Max
0,0018502
0,0016189
0,0013876
0,0011564
0,0009251
0,00069382
0,00046255
0,00023127
0 Min
B: Statisch-mechanische Analyse
Vergleichsspannung
Typ: Vergleichsspannung (von Mises)
Einheit: Pa
Zeit: 1
18.01.2017 17:43
3,0781e8 Max
2,7361e8
2,3941e8
2,0521e8
1,7101e8
1,3681e8
1,0261e8
6,8408e7
3,4208e7
7773,4 Min

Image 40. - Iteration 1

$$\sigma_{VM} > \sigma_{YA}$$

Iteration 2

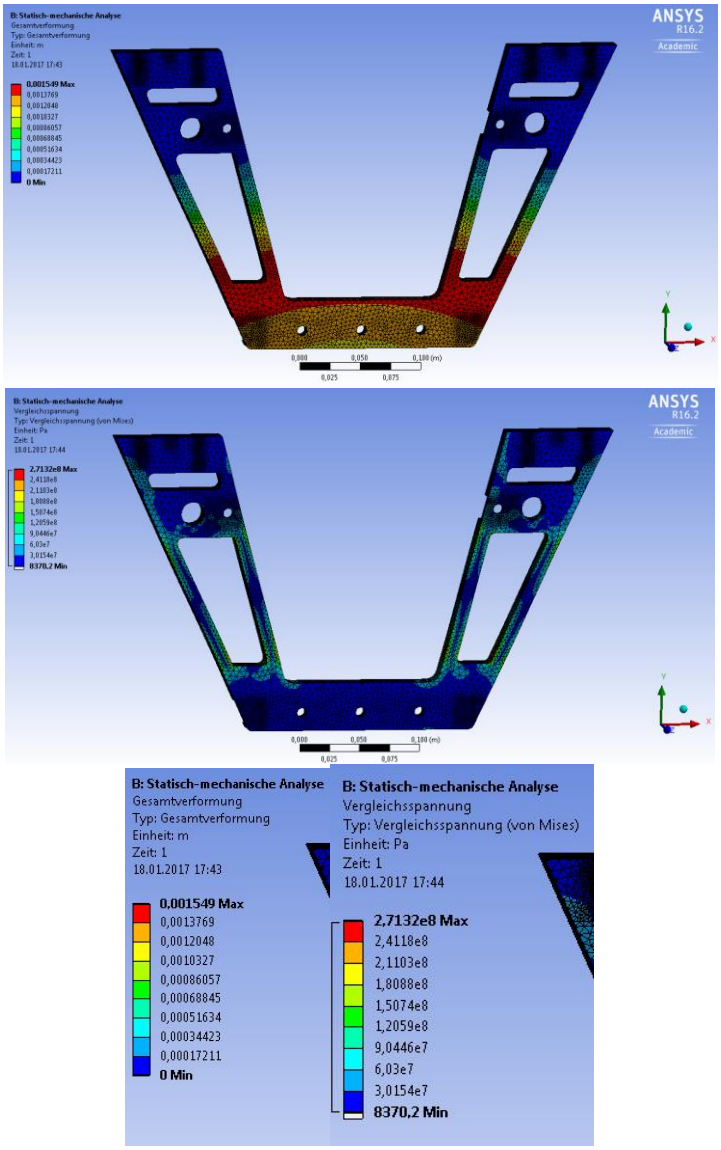

Image 41. - Iteration 2

$$Desplaz_{max} > 0.001m$$

Iteration 3

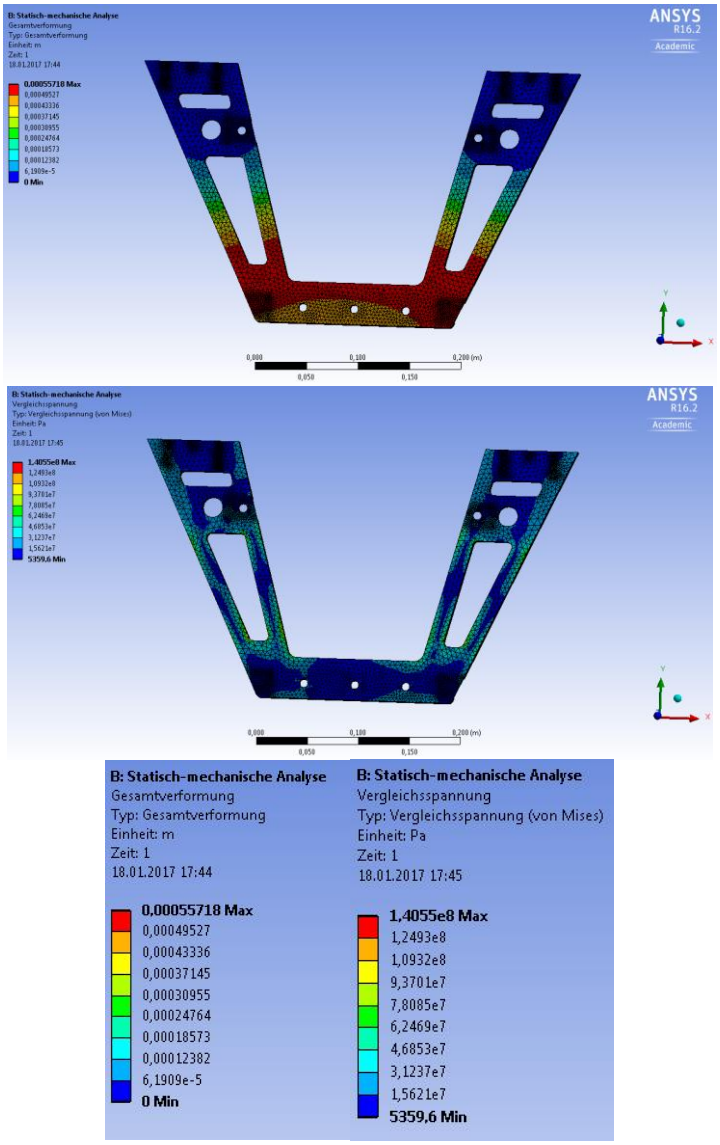

Image 42. - Iteration3

$$\sigma_{VM} < \sigma_{YA}$$
$$Desplaz_{max} < 0.001m$$

Back frame (aluminum)

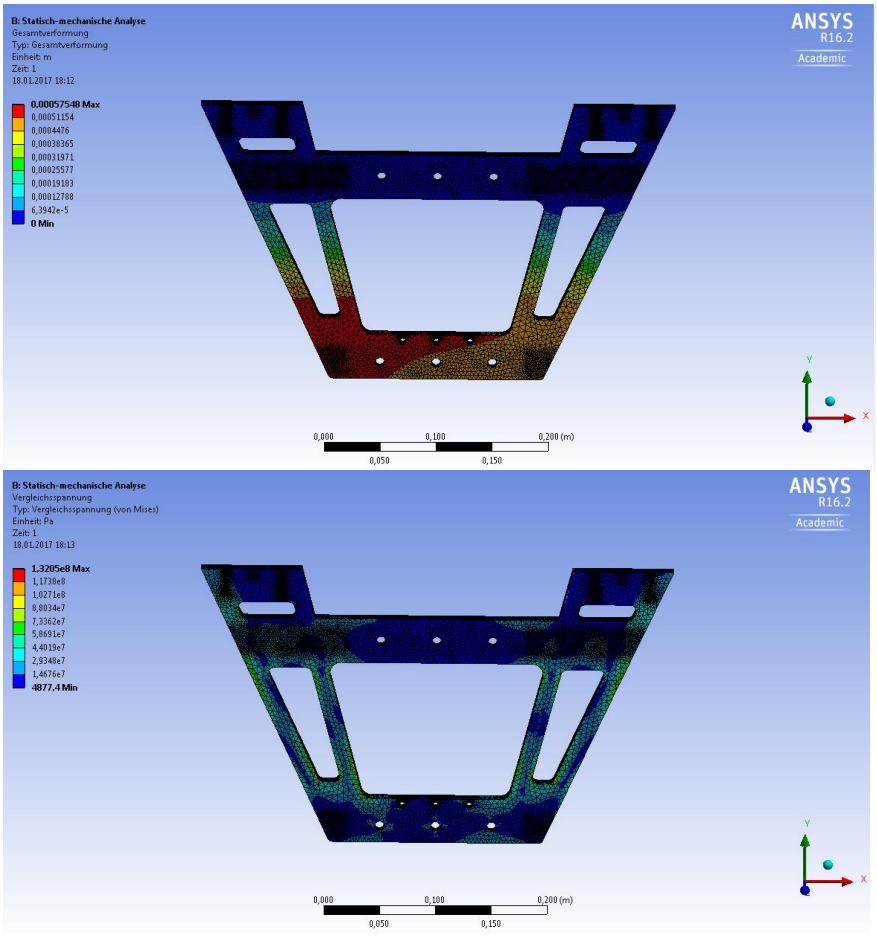

Image 43. - Simulation back frame

$$\sigma_{VM} < \sigma_Y$$
$$Desplaz_{max} < 0.001m$$

With these iterations, nearly 1kg has been reduced of the initial weight of the carriage. It is important make the design as light as possible in order to achieve later on the acceleration goal

Bolt (stainless steel)

As it was explained with the frame, it is important to explain that with these simulations helps us to give an overview of the bolt behavior with the maximum force. However the bearings which support the transversal load are not included.

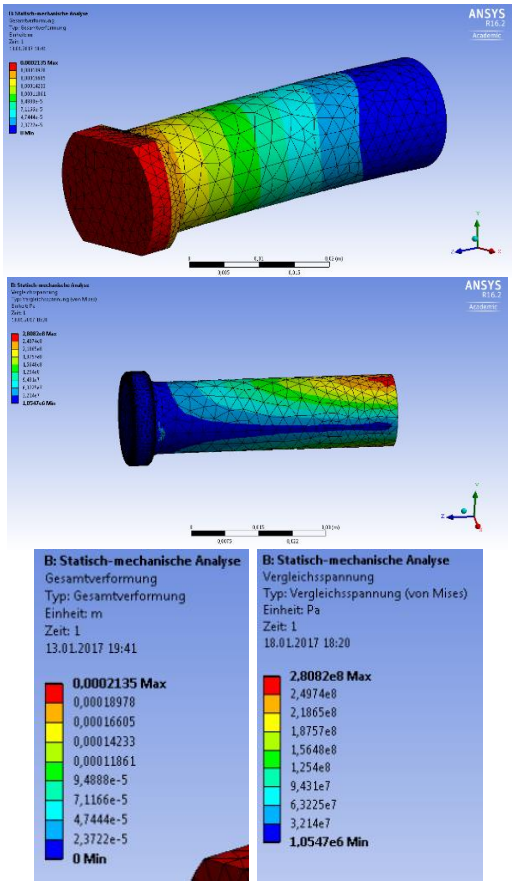

Image 44. - Bolt simulation

$$\sigma_{VM} < \sigma_Y$$
$$Desplaz_{max} < 0.001\text{mm}$$

CHAPTER 6: Conclusions and future lines.

CHAPTER 6: Conclusions and future lines.

Conclusions

This chapter is the last chapter of the document. It begins with a review of the goals that were pursued with the realization of this project, to later study the conclusions obtained. Finally, a set of future lines of research will be presented, as I am going to continue working in the present project.

In the execution of a technical project, a long process is followed since the need for the element to be projected until it is integrated into the overall process of which it forms part. The process of doing a technical project can be subdivided into different parts: idea, design, execution and evaluation. But, on the other hand, it is the nature and scope of the project that makes necessary that this process to be completed.

If it is a sufficiently well-known element of technology, the least importance of any phase of the project is understandable, or even that it can be omitted, since the design of a sufficiently proven type and absolute guarantee would undoubtedly be accepted.

However, if the modification of an existing element, such as in this case the "HiLiTe2" at the Leibniz Universität Hannover, it would only be necessary to carry out the study established in this project and the execution of it.

With the new design of the "HiLiTe2" the problems with the maximum load, pulling up and measure are solved.
This fact is sufficient reason to justify the goals set in the present project. However, the development of the project concludes that:

- The maximum normal force is 2000 N. To achieve this goal it was necessary to introduce two different bellows cylinder to get a range of loads between 100-2000 N. After looking in the market the final decision was to introduce two bellow cylinder (ADVENTICS) because they are the best options fulfilling the restrictions, as it is shown in the Annexes.

- To design a new frame for take out the bellow cylinder. Once the bellows cylinders were chosen, the next step was adapt the whole frame to make it possible. The front frame has a wide open design in order to give the possibility of easily exchange the two bellows cylinders.

- New design for pull up the chassis. The main problem was that the piston cannot pull up the chassis with the maximum compressed air and it has not enough stroke. The first step was to introduce two pistons (FESTO) with enough force to pull up the chassis and a stroke of 40 mm.

- To design a new system to support the chassis under the maximum load. This new system has a small piston which transmit the stroke to two bolts. These bolts are supported through two linear ball bearing which support the load.

- To introduce a linear transducer when tests under snow are done in order to measure the distance that the sample can be introduced into the snow. The brand of this linear transducer is WAYCON due to the fact that it was the best to achieve all the specifications. The design of a new part to introduce it into the assembly was done.

- New design for the sample holder. The goal was to make a new design in order to make it easier to remove. To achieve this goal one new part was designed which is screwed to the sample holder.

In general, this project is not only complex because of the importance of the work undertaken but also due to the numerous interconnected processes that are part of the design process and that must be satisfied to ensure the continuity of the same.

Future lines

After the design of the carriage is done, the future lines are the next step due to the fact I am going to continue with this project.

The main ideas are described in the following sections:

- **Movement of the carriage**
  - Actuator line.

    Advantages: it is possible to buy it all together.

    Disadvantages: to check if the acceleration specification can be achieved.

    Characteristics are shown in the Annexes.

    The first design is shown in the next picture.

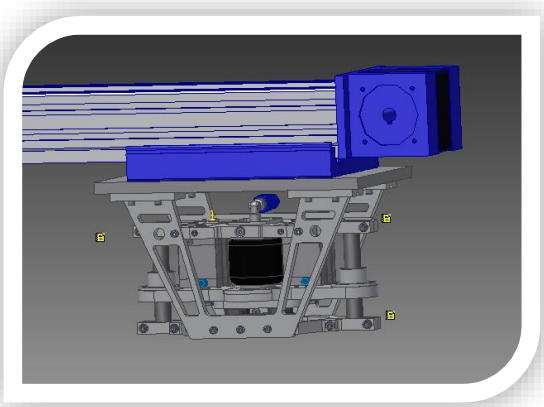

Image 45. - Actuator line. Future lines

  - Tooth Belt.

    Advantages: it can be designed to achieve all the specifications.

Disadvantages: different components.

- **Support structure**. To design a new structure to hold this linear actuator or belt.

- **Bottom structure for the path holder.**
  - New design through pistons. This idea is cheaper but not so precise.
  - Linear actuator for pull up and down the whole structure. This design is precise but expensive.

At the same time the manufacturing process is going to start.
In April I will send all the drawings to the workshop in order to manufacture all the parts while I will continue at the same time designing the new parts I explained before.
The main reason is due to the fact that I have been hired by the Leibniz Universität Hannover for 1 year.

Annexes

Annexes

A. - Drawing assemblies and codification

- Assembly drawings

Assembly	Number
HiLiTe2	0000
Carriage	1000
Frame	1100
Force Sensor assembly	1200
Bellow cylinder	1300
Block Piston	1400
Actuator line	2000

- Subassemblies drawings

➢ 1100 Frame

Name	Identifier	Units	Brand	Material
Front frame	1101	1		Aluminium 7050
Back frame	1102	1		Aluminium 7050
Foot	1103	4		Aluminium 7050
Bottom frame 1	1104	1		Aluminium 7050
Bottom frame 2	1105	1		Aluminium 7050
Top frame 1	1106	1		Aluminium 7050
Top frame 2	1107	1		Aluminium 7050
Top frame 3	1108	1		Aluminium 7050
Top frame 4	1109	1		Aluminium 7050
Chasis	1110	1		Aluminium 7050
Clamp bearing	1111	1		Aluminium 7050
Bottom Clamp bellow 95_big	1112	1		Aluminium 7050
Bottom Clamp bellow 100_small	1112	1		Aluminium 7050
Screw piston	1113	2		Aluminium 7050
Plastic cover	1114	1		Plastic
Hollow shaft	KH30	2	INNA	
Ball bearing	WH30	2	INNA	
Piston	572705_ADN-63-40-I-PPS-A	2	FESTO	
Quick connector	2028_CK-1_8-PK-6	2	FESTO	
Linear potentiometer	LZW1-F-50	1	WAYCON	
Screw	DIN 7991 - M8x30	14		
Screw	DIN 7991 - M8 x 45	1		
Screw	DIN 7991 - M4x12	8		
Screw	DIN 7991 - M6x12	1		
Screw	DIN 912 - M8 x 25	27		
Screw	DIN 912 - M8 x 40	4		
Screw	DIN 912 - M8 x 55	4		
Screw	DIN 912 - M6 x 20	2		
Screw	DIN 912 - M4 x 30	3		
Screw	DIN 912 - M3 x 12	3		
Plain washer	ISO 7091 - ST 8 - 100 HV	24		
Nut	ISO 4036 - M4(2)	1		
Pin	ISO 8734 - 6 x 16 - ADIN EN	4		

- 1200 Force sensor assembly

Name	Identifier	Units	Brand	Material
Holder 2mm	1201	1		Aluminium 7050
Holder 5mm	1201	1		Aluminium 7050
Clamp Holder 2mm	1202	1		Aluminium 7050
Clamp Holder 5mm	1202	1		Aluminium 7050
Base plate	1203	1		Aluminium 7050
Top plate	1204	1		Aluminium 7050
Bolt	1205	2		Stainless steel
Force transducer	Kistler 9047C	2	Kistler	
Nut	Kistler 9466	2	Kistler	
Screw	DIN 7991 - M8x20	4		
Screw	DIN 7991 - M8x25	3		
Screw	DIN 912 - M5 x 12	1		
Pin	ISO 8734 - 6 x 16 - ADIN EN	2		

- 1300 Bellow cylinder

Name	Identifier	Units	Brand	Material
Bellow cylinder 95	822419121	1	Adventics	
Bellow cylinder 100	822419120	1	Adventics	
Top Clamp bellow	1301	1		Aluminium 7050
Double nipple E-3.8-3.8	3578_E-3_8-3_8	1	FESTO	
Elbow fitting	8030211_NPFC-L-2G38-F	1	FESTO	
Coupling plug	151780_KSS6-3_8-A	1	FESTO	
Quick coupling socket	531654_KDS6-CK-13	1	FESTO	

- Block Piston

Name	Identifier	Units	Brand	Material
Shell	1401	1		Aluminium 7050
Stock over	1402	2		Aluminium 7050
Connector	1403	1		Aluminium 7050
Bolt	1404	2		Stainless steel
Piston	536226_ADN-16-5-I-P-A	1	FESTO	
Linear ball bearing	KH16-PP	2	INNA	
Double nipple	4138_E-M5-1_8	2	FESTO	
Elbow fitting	8030209_NPFC-L-2G18-F	2	FESTO	
Quick connector	2028_CK-1_8-PK-6	2	FESTO	
Screw	DIN 7991 - M4 x 16	5		
Screw	DIN 7991 - M6 x 20	3		
Screw	DIN 6912 M3 x 12	8		

B. - Commercial parts

Compact cylinder
ADN-63-40-I-PPS-A

FESTO

Part number: 572705
★ Core product range
with self-adjusting pneumatic end position cushioning

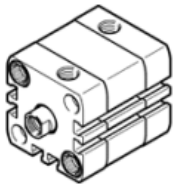

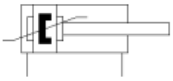

Data sheet

Feature	values
Stroke	40 mm
Piston diameter	63 mm
Piston rod thread	M10
Cushioning	PPS: Self-adjusting pneumatic end-position cushioning
Assembly position	Any
Conforms to standard	ISO 21287
Piston-rod end	Female thread
Position detection	For proximity sensor
Variants	Single-ended piston rod
Working pressure	1 ... 10 bar
Mode of operation	double-acting
Operating medium	Compressed air in accordance with ISO8573-1:2010 [7:4:4]
Note on operating and pilot medium	Lubricated operation possible (subsequently required for further operation)
Corrosion resistance classification CRC	2 - Moderate corrosion stress
Ambient temperature	-20 ... 80 °C
Impact energy in end positions	4.8 J
Cushioning length	7 mm
Theoretical force at 6 bar, return stroke	1,750 N
Theoretical force at 6 bar, advance stroke	1,870 N
Moving mass with 0 mm stroke	180 g
Additional weight per 10 mm stroke	59 g
Basic weight for 0 mm stroke	722 g

Compact cylinder
ADN-16-5-I-P-A

FESTO

Part number: 536226
★ Core product range

With position sensing and internal piston rod thread

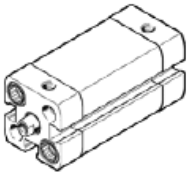

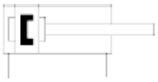

Data sheet

Feature	values
Stroke	5 mm
Piston diameter	16 mm
Piston rod thread	M4
Cushioning	P: Flexible cushioning rings/plates at both ends
Assembly position	Any
Conforms to standard	ISO 21287
Piston-rod end	Female thread
Position detection	For proximity sensor
Variants	Single-ended piston rod
Working pressure	1 ... 10 bar
Mode of operation	double-acting
Operating medium	Compressed air in accordance with ISO8573-1:2010 [7:4:4]
Note on operating and pilot medium	Lubricated operation possible (subsequently required for further operation)
Corrosion resistance classification CRC	2 - Moderate corrosion stress
Ambient temperature	-20 ... 80 °C
Impact energy in end positions	0.15 J
Theoretical force at 6 bar, return stroke	90 N
Theoretical force at 6 bar, advance stroke	121 N
Moving mass with 0 mm stroke	15 g
Additional weight per 10 mm stroke	14 g
Basic weight for 0 mm stroke	79 g
Additional mass factor per 10 mm of stroke	4 g

Linear ball bearings KH16-PP

(Series KH..-PP)

with initial greasing, sealed on both sides, with relubrication facility

F_w	16	mm	
D	24	mm	
L	30	mm	
			Shaft diameter dLw, Fase x dLw <= 10: x = 1 tolerance +1 10 < dLw <= 30: x = 1,5 tolerance +1 30 < dLw <= 80: x = 2,5 tolerance +1
J_{L4}	7	mm	
N_2	2,5	mm	
			Supplied with initial greasing (sealed on both sides)
m	27,5	g	Mass of bearing
			The basic load ratings are only valid for hardened (670+170 HV) and ground shaft raceways.
C_{min}	890	N	Basic dynamic load rating
C_0 min	620	N	Basic static load rating
C_{max}	1060	N	Basic dynamic load rating
C_0 max	910	N	Basic static load rating
			Designs with anti-corrosion protection have the suffix -RR.

Linear potentiometer:

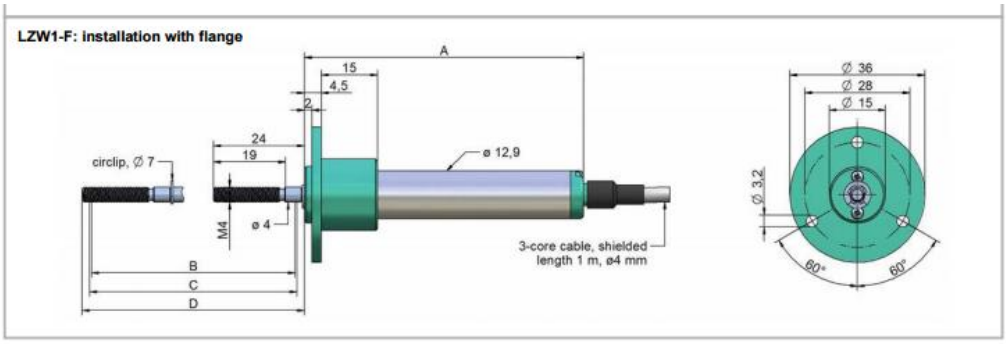

WayCon
Positionsmesstechnik

TECHNICAL DATA

Measuring range	[mm]	25 / 50 / 75 / 100 / 125 / 150 / 200 / 250
Protection class		IP60
Displacement speed	[m/s]	≤10
Displacement force	[N]	≤0.5
Resolution		Resolution depends on the signal quality of the reference voltage respectively supply voltage.
Tolerance on resistance	[%]	±20
Recommended cursor current	[µA]	<0.1
Maximum cursor current	[mA]	10
Temperature coefficient of the output voltage	[ppm/°C]	<1.5
Vibrations DIN IEC68T2-6		20 g, 5...2000 Hz
Electrical isolation		>100 MOhm at 500 V=, 1 Bar, 2 s
Dielectric strength		<100 µA at 500 V~, 50 Hz, 1 Bar, 2 s
Working temperature	[°C]	-30...+100
Storage temperature	[°C]	-50...+120
Rod material		high-grade steel AISI 303
Housing material		anodised aluminium, Nylon 66 G 25
Mounting		LZW1-S with brackets, LZW1-A with rod end bearings, LZW1-F with flange

Linear ball bearings KH30 (Series KH)

with preservative, not sealed, with relubrication facility

The datasheet is only an overview of dimensions and basic load ratings of the selected product. Please always observe all the guidelines in these overview pages. Further information is given on many products under the menu item "Description". You can also order comprehensive information via the Catalogue ordering system (http://www.ina.de/content.ina.de/en/mediathek/library/library.jsp) or by telephone on +49 (91 32) 82 - 28 97.

F_w	30	mm	
D	40	mm	
L	50	mm	
			Shaft diameter dLw, Fase x dLw <= 10: x = 1 tolerance +1 10 < dLw <= 30: x = 1,5 tolerance +1 30 < dLw <= 80: x = 2,5 tolerance +1
J_{L4}	8	mm	
N_2	2,5	mm	
			Supplied coated with a preservative
m	95	g	Mass of bearing
			The basic load ratings are only valid for hardened (670+170 HV) and ground shaft raceways.
C_{min}	3300	N	Basic dynamic load rating
$C_{0\,min}$	2700	N	Basic static load rating
C_{max}	3300	N	Basic dynamic load rating
$C_{0\,max}$	3100	N	Basic static load rating
			Designs with anti-corrosion protection have the suffix -RR.

Hollow shafts WH30 (Series WH)

hollow shafts

The datasheet is only an overview of dimensions and basic load ratings of the selected product. Please always observe all the guidelines in these overview pages. Further information is given on many products under the menu item "Description". You can also order comprehensive information via the Catalogue ordering system (http://www.ina.de/content.ina.de/en/mediathek/library/library.jsp) or by telephone on +49 (91 32) 82 - 28 97.

d	18,2	mm	Tolerance: +/-0,15
d_{LW}	30	mm	Tolerance h7: 0/-21 µm Diameter tolerance h6 available by agreement
L_{max}	7100	mm	
1)			The roundness corresponds to no more than half the diameter tolerance
2)			For shaft length < 500 mm max. straightness tolerance of 0,1 mm.
Rht_{min}	1,5	mm	Surface hardening depth: To DIN ISO 13012
t_2	9	µm	Parallelism
t_3	0,2		Straightness
mw	3,55	kg/m	Mass of shaft

ROBOT 220 SP

ROBOT 220 SP dimensions

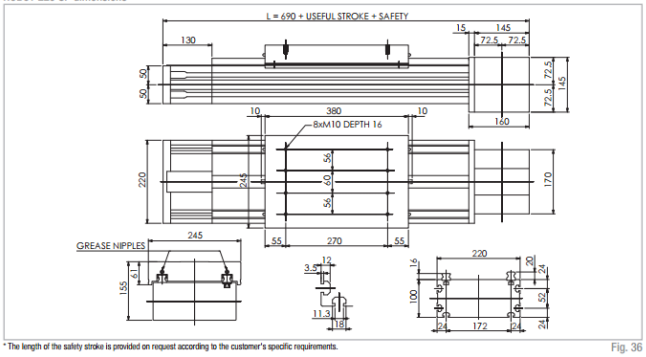

* The length of the safety stroke is provided on request according to the customer's specific requirements.

Fig. 36

Technical data

	Type
	ROBOT 220 SP
Max. useful stroke length [mm]*1	6000
Max. positioning repeatability [mm]*2	± 0.05
Max. speed [m/s]	5.0
Max. acceleration [m/s²]	50
Type of belt	100 AT 10
Type of pulley	Z 25
Pulley pitch diameter [mm]	79.58
Carriage displacement per pulley turn [mm]	250
Carriage weight [kg]	14.4
Zero travel weight [kg]	41
Weight for 100 mm useful stroke [kg]	2.5
Starting torque [Nm]	6.4
Moment of inertia of each pulley [g mm²]	4.114 · 10⁶

*1) It is possible to obtain strokes up to 11000 mm by means of special Rollon joints
*2) Positioning repeatability is dependent on the type of transmission used

Tab. 84

Moments of inertia of the aluminum body

Type	I_x [10⁷ mm⁴]	I_y [10⁷ mm⁴]	I_p [10⁷ mm⁴]
ROBOT 220	0.65	3.26	3.92

Tab. 85

Driving belt

The driving belt is manufactured from a friction resistant polyurethane and with steel cords for high tensile stress resistance.

Type	Type of belt	Belt width [mm]	Weight kg/m
ROBOT 220 SP	100 AT 10	100	0.58

Tab. 86

Belt length (mm) = 2 x L - 120

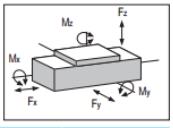

ROBOT 220 SP - Load capacity

Type	F_x [N]		F_y [N]		F_z [N]		M_x [Nm]		M_y [Nm]		M_z [Nm]	
	Stat.	Dyn.	Stat.	Dyn	Stat.	Dyn	Stat.	Dyn	Stat.	Dyn	Stat.	Dyn
ROBOT 220 SP	8510	5520	158000	110000	158000	110000	13588	9460	17696	12320	17696	12320

See verification under static load and lifetime on page SL-2 and SL-3

Tab. 87

C. - Tolerances

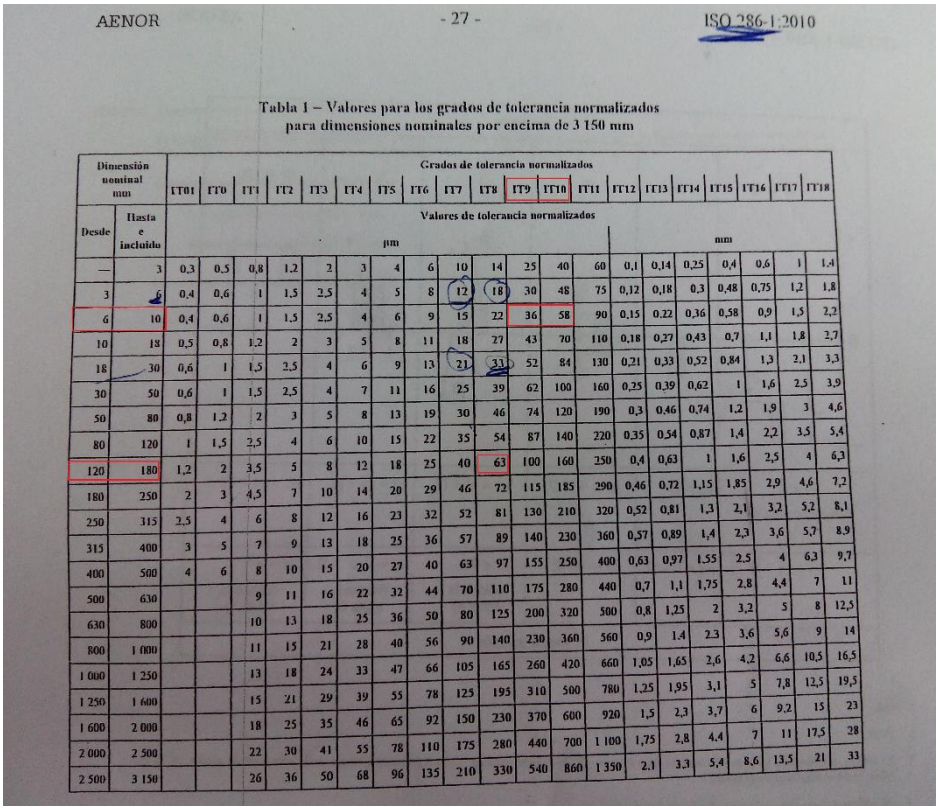

AENOR - 27 - ISO 286-1:2010

Tabla 1 – Valores para los grados de tolerancia normalizados para dimensiones nominales por encima de 3 150 mm

Dimensión nominal mm		Grados de tolerancia normalizados																		
		IT01	IT0	IT1	IT2	IT3	IT4	IT5	IT6	IT7	IT8	IT9	IT10	IT11	IT12	IT13	IT14	IT15	IT16	IT17	IT18
Desde	Hasta e incluido	Valores de tolerancia normalizados																			
		µm													mm						
—	3	0,3	0,5	0,8	1,2	2	3	4	6	10	14	25	40	60	0,1	0,14	0,25	0,4	0,6	1	1,4
3	6	0,4	0,6	1	1,5	2,5	4	5	8	12	18	30	48	75	0,12	0,18	0,3	0,48	0,75	1,2	1,8
6	10	0,4	0,6	1	1,5	2,5	4	6	9	15	22	36	58	90	0,15	0,22	0,36	0,58	0,9	1,5	2,2
10	18	0,5	0,8	1,2	2	3	5	8	11	18	27	43	70	110	0,18	0,27	0,43	0,7	1,1	1,8	2,7
18	30	0,6	1	1,5	2,5	4	6	9	13	21	33	52	84	130	0,21	0,33	0,52	0,84	1,3	2,1	3,3
30	50	0,6	1	1,5	2,5	4	7	11	16	25	39	62	100	160	0,25	0,39	0,62	1	1,6	2,5	3,9
50	80	0,8	1,2	2	3	5	8	13	19	30	46	74	120	190	0,3	0,46	0,74	1,2	1,9	3	4,6
80	120	1	1,5	2,5	4	6	10	15	22	35	54	87	140	220	0,35	0,54	0,87	1,4	2,2	3,5	5,4
120	180	1,2	2	3,5	5	8	12	18	25	40	63	100	160	250	0,4	0,63	1	1,6	2,5	4	6,3
180	250	2	3	4,5	7	10	14	20	29	46	72	115	185	290	0,46	0,72	1,15	1,85	2,9	4,6	7,2
250	315	2,5	4	6	8	12	16	23	32	52	81	130	210	320	0,52	0,81	1,3	2,1	3,2	5,2	8,1
315	400	3	5	7	9	13	18	25	36	57	89	140	230	360	0,57	0,89	1,4	2,3	3,6	5,7	8,9
400	500	4	6	8	10	15	20	27	40	63	97	155	250	400	0,63	0,97	1,55	2,5	4	6,3	9,7
500	630			9	11	16	22	32	44	70	110	175	280	440	0,7	1,1	1,75	2,8	4,4	7	11
630	800			10	13	18	25	36	50	80	125	200	320	500	0,8	1,25	2	3,2	5	8	12,5
800	1 000			11	15	21	28	40	56	90	140	230	360	560	0,9	1,4	2,3	3,6	5,6	9	14
1 000	1 250			13	18	24	33	47	66	105	165	260	420	660	1,05	1,65	2,6	4,2	6,6	10,5	16,5
1 250	1 600			15	21	29	39	55	78	125	195	310	500	780	1,25	1,95	3,1	5	7,8	12,5	19,5
1 600	2 000			18	25	35	46	65	92	150	230	370	600	920	1,5	2,3	3,7	6	9,2	15	23
2 000	2 500			22	30	41	55	78	110	175	280	440	700	1 100	1,75	2,8	4,4	7	11	17,5	28
2 500	3 150			26	36	50	68	96	135	210	330	540	860	1 350	2,1	3,3	5,4	8,6	13,5	21	33

Tabla 19 – Desviaciones límite para ejes (desviaciones fundamentales e y ef)
Desviación límite superior = *es*
Desviación límite inferior = *ei*

Desviaciones en micrómetros

Dimensión nominal mm		e						ef[a]							
Desde	Hasta e incluido	5	6	7	8	9	10	3	4	5	6	7	8	9	10
—	3	−14 −18	−14 −20	−14 −24	−14 −28	−14 −39	−14 −54	−10 −12	−10 −13	−10 −14	−10 −16	−10 −20	−10 −24	−10 −35	−10 −50
3	6	−20 −25	−20 −28	−20 −32	−20 −38	−20 −50	−20 −68	−14 −16,5	−14 −18	−14 −19	−14 −22	−14 −26	−14 −32	−14 −44	−14 −62
6	10	−25 −31	−25 −34	−25 −40	−25 −47	−25 −61	−25 −83	−18 −20,5	−18 −22	−18 −24	−18 −27	−18 −33	−18 −40	−18 −54	−18 −76
10	18	−32 −40	−32 −43	−32 −50	−32 −59	−32 −75	−32 −102								
18	30	−40 −49	−40 −53	−40 −61	−40 −73	−40 −92	−40 −124								
30	50	−50 −61	−50 −66	−50 −75	−50 −89	−50 −112	−50 −150								
50	80	−60 −73	−60 −79	−60 −90	−60 −106	−60 −134	−60 −180								
80	120	−72 −87	−72 −94	−72 −107	−72 −126	−72 −159	−72 −212								
120	180	−85 −103	−85 −110	−85 −125	−85 −148	−85 −185	−85 −245								
180	250	−100 −120	−100 −129	−100 −146	−100 −172	−100 −215	−100 −285								
250	315	−110 −133	−110 −142	−110 −162	−110 −191	−110 −240	−110 −320								
315	400	−125 −150	−125 −161	−125 −182	−125 −214	−125 −265	−125 −355								
400	500	−135 −162	−135 −175	−135 −198	−135 −232	−135 −290	−135 −385								
500	630		−145 −189	−145 −215	−145 −255	−145 −320	−145 −425								
630	800		−160 −210	−160 −240	−160 −285	−160 −360	−160 −480								
800	1 000		−170 −226	−170 −260	−170 −310	−170 −400	−170 −530								
1 000	1 250		−195 −261	−195 −300	−195 −360	−195 −455	−195 −615								
1 250	1 600		−220 −298	−220 −345	−220 −415	−220 −530	−220 −720								
1 600	2 000		−240 −332	−240 −390	−240 −470	−240 −610	−240 −840								
2 000	2 500		−260 −370	−260 −435	−260 −540	−260 −700	−260 −960								
2 500	3 150		−290 −425	−290 −500	−290 −620	−290 −830	−290 −1 150								

[a] La desviación fundamental intermedia ef se utiliza principalmente para mecanismos finos y horología. Si se requieren las clases de tolerancia que incluye la desviación fundamental en otras dimensiones nominales, deben calcularse según la Norma ISO 286-1.

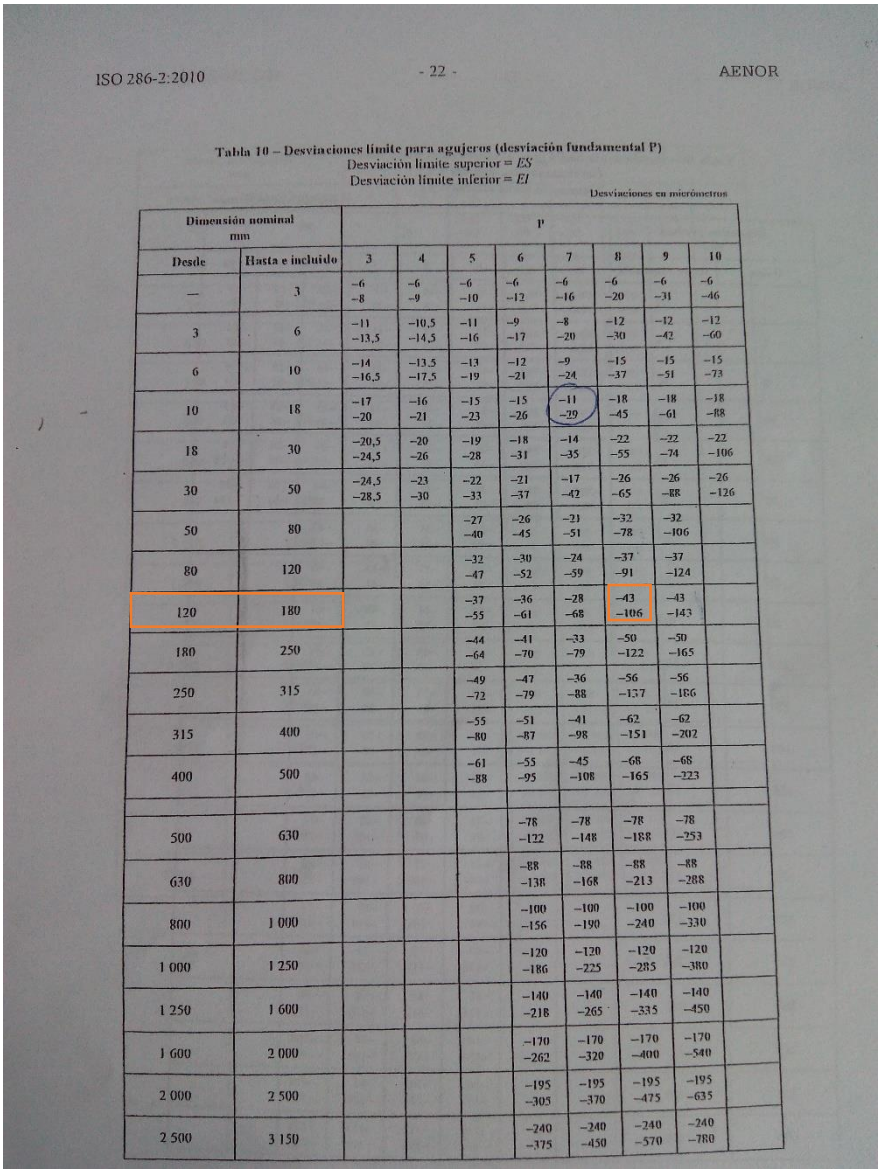

ISO 286-2:2010 - 22 - AENOR

Tabla 10 – Desviaciones límite para agujeros (desviación fundamental P)
Desviación límite superior = *ES*
Desviación límite inferior = *EI*

Desviaciones en micrómetros

Dimensión nominal mm		P							
Desde	Hasta e incluido	3	4	5	6	7	8	9	10
—	3	−6 −8	−6 −9	−6 −10	−6 −12	−6 −16	−6 −20	−6 −31	−6 −46
3	6	−11 −13,5	−10,5 −14,5	−11 −16	−9 −17	−8 −20	−12 −30	−12 −42	−12 −60
6	10	−14 −16,5	−13,5 −17,5	−13 −19	−12 −21	−9 −24	−15 −37	−15 −51	−15 −73
10	18	−17 −20	−16 −21	−15 −23	−15 −26	−11 −29	−18 −45	−18 −61	−18 −88
18	30	−20,5 −24,5	−20 −26	−19 −28	−18 −31	−14 −35	−22 −55	−22 −74	−22 −106
30	50	−24,5 −28,5	−23 −30	−22 −33	−21 −37	−17 −42	−26 −65	−26 −88	−26 −126
50	80			−27 −40	−26 −45	−21 −51	−32 −78	−32 −106	
80	120			−32 −47	−30 −52	−24 −59	−37 −91	−37 −124	
120	180			−37 −55	−36 −61	−28 −68	−43 −106	−43 −143	
180	250			−44 −64	−41 −70	−33 −79	−50 −122	−50 −165	
250	315			−49 −72	−47 −79	−36 −88	−56 −137	−56 −186	
315	400			−55 −80	−51 −87	−41 −98	−62 −151	−62 −202	
400	500			−61 −88	−55 −95	−45 −108	−68 −165	−68 −223	
500	630				−78 −122	−78 −148	−78 −188	−78 −253	
630	800				−88 −138	−88 −168	−88 −213	−88 −288	
800	1 000				−100 −156	−100 −190	−100 −240	−100 −330	
1 000	1 250				−120 −186	−120 −225	−120 −285	−120 −380	
1 250	1 600				−140 −218	−140 −265	−140 −335	−140 −450	
1 600	2 000				−170 −262	−170 −320	−170 −400	−170 −540	
2 000	2 500				−195 −305	−195 −370	−195 −475	−195 −635	
2 500	3 150				−240 −375	−240 −450	−240 −570	−240 −780	

Bibliography

Books:

1. Solid Modelling and CAD Systems: How to Survive a CAD System (Stroud, Ian.)
2. Introduction to Autodesk Inventor 2013 and Autocad 2013. (Randy Shih)
3. Dimensioning and tolerancing handbook (Drake, Paul J.)
4. Finite element analysis : From concepts to applications (David S. Burnett)
5. Finite element modeling for stress analysis (Robert D. Cook)
6. Engineering materials : properties and selection (Budinski, Kenneth G.)
7. Materials selection for engineering design (Mahmoud M. Farag)
8. Diagnóstico y corrección de fallos de componentes mecánicos (Besa Gonzálvez, Antonio José)
9. Machine Tools for High Performance Machining (López de Lacalle, L.N.)

Web pages:

1. Festo: https://www.festo.com/cms/de_de/index.htm
2. INA: http://www.ina.de/content.ina.de/en/
3. Kistler: https://www.kistler.com/de/de/
4. Wayon: http://www.waycon.de/
5. https://en.wikipedia.org/wiki/Von_Mises_yield_criterion